

dynamAedes: a unified modelling framework for invasive *Aedes* mosquitoes

Daniele Da Re^{1,*}, Wim Van Bortel², Friederike Reuss^{3,4},
Ruth Müller², Sebastien Boyer⁵, Fabrizio Montarsi⁶,
Silvia Ciocchetta⁷, Daniele Arnoldi⁸, Giovanni Marini⁸,
Annapaola Rizzoli⁸, Gregory L'Amber⁹,
Guillaume Lacour¹⁰, Constantianus J.M. Koenraadt¹¹,
Sophie O. Vanwambeke^{1,†}, Matteo Marcantonio^{12,†}

21st December 2021

¹ Georges Lemaître Center for Earth and Climate Research, Earth and Life Institute, UCLouvain, Louvain-la-Neuve, Belgium

² Unit Entomology and the Outbreak Research Team, Tropical Medicine Institute, Antwerp, Belgium

³ Senckenberg Biodiversity and Climate Research Centre, Frankfurt am Main, Germany

⁴ Institute of Occupational, Social and Environmental Medicine, Goethe University, Frankfurt am Main, Germany

⁵ Medical and Veterinary Entomology Unit, Institute Pasteur du Cambodge, Cambodia

⁶ Laboratory of Parasitology, National reference centre/OIE collaborating centre for diseases at the animal-human interface, Istituto Zooprofilattico Sperimentale delle Venezie, Legnaro, Italy

⁷ The University of Queensland, School of Veterinary Science, Gatton, Australia

⁸ Department of Biodiversity and Molecular Ecology, Research and Innovation Centre, Fondazione Edmund Mach, San Michele all'Adige, Trento, Italy

⁹ EID Méditerranée, Direction Technique, Montpellier, France

¹⁰ Altopictus, Pérols, France

¹¹ Wageningen University & Research, Department of Plant Sciences, Laboratory of Entomology, Wageningen, The Netherlands.

¹² Evolutionary Ecology and Genetics Group, Earth and Life Institute, UCLouvain, Louvain-la-Neuve, Belgium

* corresponding author: daniele.dare@uclouvain.be

† SOV and MM equally supervised the project

Abstract

- 1 1. Mosquito species belonging to the genus *Aedes* have attracted the interest of
2 scientists and public health officers for their invasive species traits and efficient
3 capacity of transmitting viruses affecting humans. Some of these species were
4 brought outside their native range by human activities such as trade and tourism,
5 and colonised new regions thanks to a unique combination of eco-physiological
6 traits.
- 7 2. Considering mosquito physiological and behavioural traits to understand and
8 predict the spatial and temporal population dynamics is thus a crucial step to
9 develop strategies to mitigate the local densities of invasive *Aedes* populations.
- 10 3. Here, we synthesised the life cycle of four invasive *Aedes* species (*Ae. aegypti*,
11 *Ae. albopictus*, *Ae. japonicus* and *Ae. koreicus*) in a single multi-scale stochas-
12 tic modelling framework which we coded in the R package `dynamAedes`. We
13 designed a stage-based and time-discrete stochastic model driven by tempera-
14 ture, photo-period and inter-specific larval competition that can be applied to
15 three different spatial scales: punctual, local and regional. These spatial scales
16 consider different degrees of spatial complexity and data availability, by ac-
17 counting for both active and passive dispersal of mosquito species as well as
18 for the heterogeneity of the input temperature data.
- 19 4. Our overarching aim was to provide a flexible, open-source and user-friendly
20 tool rooted in the most updated knowledge on species biology which could be
21 applied to the management of invasive *Aedes* populations as well as for more
22 theoretical ecological inquiries.

23
24 **Keywords:** Biological invasions; Invasion ecology; Process-based models; Spa-
25 tial epidemiology; Dispersal; Vector-borne pathogens

26 **1 Introduction**

27 Some mosquito species within the *Aedes* taxon have a unique combination of biological
28 traits such as: 1) efficient transmission of viruses debilitating for humans and animals
29 (Gratz, 2004; Hurk et al., 2011; Souza-Neto et al., 2019), 2) eco-physiological plasticity
30 that allows for rapid adaptation (Kramer et al., 2021) and exploitation of novel environ-
31 ments created by humans (McBride et al., 2014a), 3) egg stage with high resistance to dry
32 and cold conditions which facilitate displacements over long ecological and geographi-
33 cal distances (Thomas et al., 2012; Versteirt et al., 2012; Kaufman and Fonseca, 2014).
34 Some of these species were accidentally brought outside their native areas by human ac-
35 tivities and colonised new regions thanks to a unique combination of eco-physiological
36 traits. These mosquitoes, often referred as "*Aedes* invasive mosquitoes" (AIM), have at-
37 tracted the interest of scientists and public health officers and much effort has been done to
38 unravel their physiological and behavioural traits. Among these species, *Ae. aegypti*, *Ae.*
39 *albopictus*, *Ae. japonicus* and *Ae. koreicus* showed a rapid expansion of their geographical
40 range, with the first two species often causing an important burden on public health. As
41 a consequence, large experimental and observational datasets on the relationship between
42 water or air temperature and physiological parameters have been collected and used to
43 develop mechanistic models that reproduce the basic life cycle of these four species (e.g.,
44 for *Ae. aegypti* Focks et al., 1993a,b; Otero et al., 2006; Da Re et al., 2021; Caldwell et al.,
45 2021; for *Ae. albopictus* Tran et al., 2013; Erguler et al., 2016; Metelmann et al., 2019;
46 Pasquali et al., 2020; Tran et al., 2020; for *Ae. japonicus* Wieser et al., 2019; for *Ae. kor-*
47 *ericus* Marini et al., 2019b). The inclusion of such functions, which describe physiological
48 and developmental rates, into modelling frameworks allow for more reliable model extrap-
49 olations, as the chances of biological unrealistic outcome may be lower compared to pure
50 correlative model approaches (Kearney, 2006; Kearney and Porter, 2009). Comparisons
51 between modelled and observed population trends showed that such mechanistic models
52 can be used, for example, to understand population dynamics in space and time, and thus
53 can enhance the pest control strategies against AIM (Baldacchino et al., 2015).

54 Models targeting AIM developed so far aimed to simulate the population dynamics
55 of only one species at the time and for a single qualitative (i.e. "individual", "container"
56 or "household") or quantitative (cell in a lattice grid) spatial scale. Moreover, only a few
57 of these models have been made readily operational, for example by organising them in
58 open-access, user-friendly software or libraries with sufficient documentation for practi-
59 cal applications (Stallman, 1985). SkeeterBuster, a container-level population dynamical
60 model for *Ae. aegypti*, has been the first agent-based model for mosquitoes made available
61 as a free (but not open-source) software (Magori et al., 2009). Concerning *Ae. albopictus*,
62 Erguler et al. (2016) made available a model developed as a Python library that was after-

63 wards wrapped into the R package `albopictus`. More recently, the European Centre
64 for Disease Control (ECDC) has provided a free and open-source adaptation of a model
65 initially developed by Tran et al. (2013), making it accessible via the R Shiny application
66 `AedesRisk`¹. Similarly, two generic age and stage-structured discrete-time population
67 dynamics models, also applicable to mosquitoes, were proposed in the last few years:
68 `stagePop` (Kettle and Nutter 2015; applied to *Ae. japonicus* in Wieser et al. 2019) and
69 `sPop` (Erguler, 2018). Despite the current availability of models applicable to invasive
70 *Aedes*, none of them can be directly generalised while retaining biological credibility, e.g.
71 species-specific models work only for a single species whereas generic models may over-
72 simplify the life cycle structure or are not equipped with species-specific physiological
73 parameters. Hence, if users decide to use generic models, they need to screen the scientific
74 literature, filter and manipulate experimental data (often scarce and non-standardised)
75 to inform models on the species of interest. Moreover, often models do not consider
76 mosquito dispersal or even completely lack spatial structure.

77 Here, we synthesised the life cycle of four AIM species: *Ae. aegypti*, *Ae. albopictus*,
78 *Ae. japonicus* and *Ae. koreicus* in a single modelling framework, which we coded in
79 the R package `dynamAedes`. We designed a stage-based and time discrete stochastic
80 model informed by temperature and photoperiod that can be applied to three different
81 spatial scales: punctual, local and regional. These spatial scales were thought to meet
82 different degrees of spatial complexity and data availability, by accounting for both active
83 and human-mediated passive dispersal of the modelled mosquito species as well as for
84 the heterogeneity of temperature data. Our overarching aim was to provide a flexible and
85 open-source tool which could be used for applications related to the management of AIM
86 populations but also for more theoretical ecological inquiries. We described and assessed
87 the model using observational mosquito data and then showed how to use the R package
88 with coding examples and relevant case studies.

89 **2 Materials and methods**

90 **2.1 A summary of invasive *Aedes* species ecology**

91 **2.1.1 *Aedes aegypti***

92 *Aedes (Stegomyia) aegypti* (Linnaeus, 1762), commonly referred to as the "yellow fever
93 mosquito", was progressively brought outside sub-Saharan Africa by human trade. It was
94 first introduced in the Americas during the 16th century and afterwards to tropical and tem-
95 perate regions of Asia and Oceania (Powell et al., 2013). Its invasion was likely favoured

¹AedesRisk v1.0: <https://shinyapps.ecdc.europa.eu/shiny/AedesRisk/>

96 by a series of functional traits, such as egg desiccation-resistance, that allows them to
97 withstand dry conditions for months, and egg moderate resistance to cold temperatures
98 (Juliano et al., 2002; Thomas et al., 2012; Kramer et al., 2020). *Aedes aegypti* efficiently
99 transmit several viruses to humans, including yellow fever, dengue, chikungunya, Zika,
100 Rift Valley, Mayaro and eastern equine encephalitis viruses (Leta et al., 2018; Näslund
101 et al., 2021; da Silva Neves et al., 2021). This is the result of several eco-evolutionary
102 traits that are specific to the species: i) high preference for human hosts (anthropophily),
103 which is channelled by genetic traits linked to behavioural and physiological evolution-
104 ary advantages (Harrington et al., 2001; McBride et al., 2014b), ii) exploitation of human
105 dwellings and architectures as shelter, hide and resting indoor sites (endophily) to avoid
106 unfavourable environmental conditions (Dzul-Manzanilla et al., 2017; Gloria-Soria et al.,
107 2018), and iii) selection of artificial containers for oviposition and subsequent larval de-
108 velopment (eusynantrophy; Christophers, 1960).

109 **2.1.2 *Aedes albopictus***

110 *Aedes (Stegomyia) albopictus* (Skuse, 1895), commonly referred as the "Asian tiger mosquito",
111 is native of tropical and subtropical regions of Southern-East Asia and Indonesia (Wat-
112 son, 1967; Hawley, 1988). It is a competent vector of several viruses, including dengue,
113 chikungunya, Zika, West Nile, eastern equine encephalitis and La Crosse viruses (Koch
114 et al., 2016; McKenzie et al., 2019; Takken and van den Berg, 2019) and it was implicated
115 as the vector species causing local transmission of dengue, chikungunya or Zika virus,
116 even at temperate latitudes outside its native distributional range (Effler et al., 2005; Rezza
117 et al., 2007; Delatte et al., 2008; Venturi et al., 2017; Brady and Hay, 2019; Giron et al.,
118 2019; Barzon et al., 2021). This species is a more opportunistic feeder compared to *Ae.*
119 *aegypti* (Cebrián-Camisón et al., 2020). It prefers sub-urban habitats with the presence
120 of vegetation, dispersing bites among several species, a behaviour that might decrease the
121 probability of pathogen transmission to humans (Turell et al., 1994; Lounibos and Kramer,
122 2016). Populations of this species located at temperate latitudes show: i) an adaptation to
123 temperate climatic conditions (Marini et al., 2020) and ii) a stronger tendency to laying
124 diapausing eggs at the end of summer (Hawley et al., 1989; Lacour et al., 2015). Dia-
125 pausing eggs have been found to be resistant to below-freezing temperatures and probably
126 allowed *Ae. albopictus* populations to overwinter and spread towards higher latitudes than
127 *Ae. aegypti* (Hawley et al., 1989; Thomas et al., 2012).

128 **2.1.3 *Aedes japonicus japonicus***

129 *Aedes (Hulecoeteomyia) japonicus japonicus* (Theobald, 1901) [*Hulecoeteomyia japon-*
130 *ica*], the "Asian bush mosquito", originated in an area comprised between East China,

131 East Russia and Japan (Tanaka et al., 1979a). This species may be competent for the trans-
132 mission of pathogens of medical importance for humans, such as dengue, West Nile, Zika
133 and Usutu viruses, but only experimental evidences of its role as vector exist (Takashima
134 and Rosen, 1989; Scott, 2003; Schaffner et al., 2011; Westby et al., 2015; Veronesi et al.,
135 2018; Jansen et al., 2018; Martinet et al., 2019; De Carlo et al., 2020; Abbo et al., 2020;
136 Hopkins et al., 2020; but see Kilpatrick et al., 2005 for an estimated risk of transmitting
137 WNV by this species). Its likely lesser role as a vector for human pathogens may also be
138 assumed from the tendency to feed on other species than humans as well as the preference
139 for more natural over urbanised areas. Established populations of *Ae. japonicus* were de-
140 tected in North America from 1998 and more recently in European countries (Scott, 2003;
141 Versteirt et al., 2009; Seidel et al., 2016; Eritja et al., 2019; Müller et al., 2020; ECDC,
142 2021). This species is well adapted to cold climates, overwintering either as larvae in the
143 warmer areas, or as diapausing eggs (Krupa et al., 2021) in areas where larval habitats
144 freeze completely (Scott, 2003; Reuss et al., 2018; Day et al., 2020).

145 **2.1.4 *Aedes koreicus***

146 *Aedes (Hulecoeteomyia) koreicus* (Edwards, 1917) [*Hulecoeteomyia koreica*] commonly
147 referred to as the "Korean bush mosquito" is native to temperate areas of Northeast Asia
148 comprising Russia, the Korean peninsula, Japan and north-east China (Tanaka et al., 1979b).
149 This species is a suspected vector of *Dirofilaria immitis*, Japanese encephalitis and chikun-
150 gunya viruses, but it has not yet been directly implicated in transmission events of zoonotic
151 pathogens (Tanaka et al., 1979b; Montarsi et al., 2015a; Ciocchetta et al., 2018). *Aedes*
152 *koreicus* is adapted to temperate climates (Versteirt et al., 2012) and has recently colonised
153 areas of Central Europe while continuing its range expansion (Capelli et al., 2011; Versteirt
154 et al., 2012; Montarsi et al., 2015a; Marcantonio et al., 2016; Werner et al., 2016; Negri
155 et al., 2021; Horváth et al., 2021; Andreeva et al., 2021; Gradoni et al., 2021; ECDC, 2021).
156 *Aedes koreicus* seems to prefer rural over highly urbanised habitats and has been found to
157 feed on other species than humans (Montarsi et al., 2013, 2014; Cebrián-Camisón et al.,
158 2020). In areas where *Ae. koreicus* lives in sympatry with other invasive *Aedes* species,
159 the Korean bush mosquito is able to colonise higher altitudes and its development can start
160 earlier in the season with respect to other AIM (Montarsi et al., 2015a; Marcantonio et al.,
161 2016). This trait may give them a competitive advantage over other container-breeding
162 mosquitoes whose adults emerge later in the season.

163 2.2 The theoretical structure of the model

164 The basic structure of `dynamAedes` has been described in Da Re et al. (2021). We
165 amended some components of the model to generalise its structure. Thus, we provide here
166 a short recap of model structure while describing the new model features.

167 `dynamAedes` is composed of three main compartments (life stages) that represent a
168 simplified version of *Aedes* the mosquito life cycle: egg, juvenile and adult stages (Fig. 1).
169 Larval and pupal stages, which can be assumed to have somewhat similar physiological
170 requirements, are fused in a unique "juvenile" compartment. Each compartment is divided
171 into sub-compartments to account for the different physiological states for individuals in
172 the three main compartments (e.g. 1-day old adult females that are not sexually mature).
173 The number of sub-compartments into each compartment is dictated by the known min-
174 imum number of days needed by each species to pass to the next stage or complete the
175 gonotrophic cycle (for adults). Thus, the minimum duration of development in each com-
176 partment varies among developmental stages as well as among species. As an example,
177 the whole duration of the developmental cycle (i.e. from egg-laying to adult emergence)
178 has a minimum duration of 11 days for *Ae. aegypti* and *Ae. albopictus*, whereas 21 days
179 for *Ae. koreicus* and *Ae. japonicus* (see Tab S3 in SM for generic model assumptions).

180 In the model, time is treated as a discrete quantity and "day" is the fundamental tempo-
181 ral unit. Therefore, each event in the simulated life cycle occurs once per day and always
182 in the same order. The model can be run with or without a spatial structure. If the model
183 is spatially explicit, space is treated as a discrete quantity. In this case, the fundamental
184 spatial unit is a (user defined) cell of a lattice grid into which the species life cycle takes
185 place and, if relevant (see below), among which adult mosquitoes disperse.

186 Adult female mosquitoes lay non-diapausing eggs, E , in the summer months or dia-
187 pausing eggs, E_d , at the end of the season. The embryonic development and hatching of
188 diapausing eggs are activated by increasing daily temperature and photoperiod (typically
189 at the end of winter or early spring). All the developmental and reproductive events con-
190 sidered in the model were treated as stochastic processes with probabilities derived from
191 temperature(or photoperiod)-dependent functions by following the generic formulation:

$$X_{s,t}^{event} \sim Binomial(X_{s,t-1}, \pi_X) \quad (1)$$

192 where $X_{s,t-1}$ may represent eggs, juveniles or adults that undergo one of the following
193 events in the life cycle: lay eggs, hatch, emerge or survive in cell s , at the end of the day
194 $t - 1$. π_X is the temperature-dependent (or photoperiod dependent for the hatching of
195 diapausing eggs) daily probability of any of the life cycle events X . All the temperature-
196 dependent functions were calibrated using data from the scientific literature (see Tab S4 in
197 SM) fitted using exponential, polynomial equations, and non-linear Beta density functions,

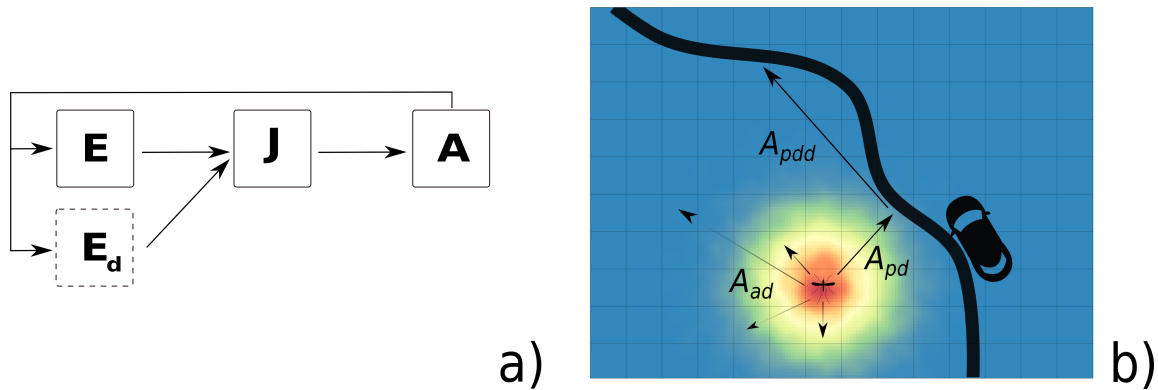


Figure 1: Graphical representation of `dynamAedes` model structure, adapted from Da Re et al. (2021): a) the life cycle of a generic simulated mosquito species, while in b) a representation of active and passive dispersal processes happening within the Adult (A) compartment at local scale. E: egg compartment; E_d : diapause egg compartment (available for all species except *Ae. aegypti*); J: juvenile compartment; A: adult compartment; A_{ad} : adult active dispersal; A_{pdd} : adult passive dispersal; A_{pd} : adult probability of being caught in a car.

198 using a combination of `drc` (non-linear models) and `aomisc` (Beta function self-starters)
199 R packages (Ritz et al., 2015; Onofri, 2020). The beta function derives from the beta
200 density function and it has been adapted to describe phenomena taking place only within a
201 minimum and a maximum threshold value (threshold model), such as physiological rates
202 with respect to temperatures in the mosquito life cycle (Onofri, 2020). In a similar fashion,
203 adult active dispersal was modelled as species-specific log-normal decaying functions of
204 distances derived from dispersal estimates from field observations for *Ae. aegypti* and *Ae.*
205 *albopictus* (Roche et al. 2015; Marcantonio et al. 2019; Marini et al. 2019a; Müller et al.
206 2020; see Tab S5 in SM for dispersal parameters). In addition to active dispersal, the model
207 also considers dispersal aided by cars along the main road network (a matrix containing
208 the coordinates of the grid cells of the landscape intersecting the road network must be
209 provided, see the "Spatial scales of the model and temperature data sources" section),
210 defined as the "hitchhiking" probability of a female to enter in a car and to be driven
211 and released further away. This probability has been defined for all species by estimates
212 measured for *Ae. albopictus* (Eritja et al., 2017), while the average distance covered by a
213 single car trip was taken from Pasaoglu et al. (2012). This type of dispersal is thought to
214 be amongst the main drivers of medium-range geographical expansion for invasive *Aedes*
215 mosquitoes, especially for *Ae. aegypti* and *Ae. albopictus* (Marcantonio et al., 2016; Eritja
216 et al., 2017; Müller et al., 2020).

217 Density-dependent survival is an important regulatory factor of mosquito population
218 dynamics (Gilpin and McClelland, 1979). Its regulatory effect for juvenile stages appears
219 to be more common in mosquitoes breeding in container or highly ephemeral habitats
220 (Juliano, 2007), such as invasive *Aedes*. In `dynamAedes` we parameterised a density-
221 dependent function by extracting observations on *Ae. aegypti* from Figures 2a and 2b in
222 Hancock et al. (2016) using the Webplot Digitizer (Rohatgi, 2020). We considered the pro-
223 portion of juveniles that survived through the juvenile stage (in a 2 L container) reported
224 by these authors as an estimate of juvenile survival probability at different densities. Mor-
225 tality probabilities ($1 - \textit{proportion surviving}$) were converted into rates, which were
226 scaled to a daily time step dividing by the corresponding immature development time (in
227 days) at different densities. Finally, we regressed the natural logarithms of these daily
228 mortality rates on the corresponding densities. The fitted daily survival rate at different
229 densities was then summed to the temperature-dependent juvenile mortality. The resulting
230 probability was then used to inform a binomial random draw (see equation 1) describing
231 overall juvenile daily survival.

232 Some invasive *Aedes* can lay eggs resistant to low temperature commonly referred
233 to as "diapausing eggs" (Thomas et al., 2012; Lacour et al., 2015; Krupa et al., 2021).
234 Diapause describes the evolutionary adaptation exploited by insect species to overcome
235 unfavourable environmental conditions by passing through an alternative and dormant
236 physiological stage. In *Ae. albopictus*, maternal photoperiod is the environmental stim-
237 ulus implied to induce oviposition of "diapausing eggs" (Pumpuni et al., 1992; Lacour
238 et al., 2015). In `dynamAedes`, the oviposition of diapausing/non-diapausing eggs was
239 integrated as a species-specific exponential function on the incidence of diapausing eggs
240 given photoperiod length (and thus geographically-dependent; Urbanski et al. 2012; Petrić
241 et al. 2021). The function is based on data from Lacour et al. (2015) for *Ae. albopictus* and
242 Krupa et al. (2021) for *Ae. japonicus*. We applied the same diapausing function developed
243 for *Ae. japonicus* to *Ae. koreicus* due to the close phylogeny of these species and the lack
244 of data for *Ae. koreicus* (see Tab. S6). The daily survival of diapausing eggs was set to
245 be constant (0.99) only for *Ae. japonicus* and *Ae. koreicus*, while for *Ae. albopictus* we
246 used the exponential function described in Metelmann et al. (2019). The hatching rate
247 of diapause eggs was triggered by an increasing photoperiod regime (spring) from 11.44
248 hours of light for *Ae. albopictus* (95th percentile estimated from Petrić et al. 2021) and
249 10.71 hours for *Ae. japonicus* or *Ae. koreicus* (Krupa et al., 2021).

250 **2.3 Overview of the R package**

251 The function `dynamAedes.m` calls the model and allows to customise the simulated sce-
252 nario through a suite of options. As for the simplest application of the model (no explicit

253 spatial dimension, `scale="ws"`, see next paragraph for further details), the user has to
254 define what species to model through the argument `species` (default `"aegypti"`), the
255 "type" and number of introduced propagules through `intro.eggs`, `intro.juvenile`
256 or `intro.adults` (default `intro.eggs=100`, `intro.juvenile=0`, `intro.adults=0`),
257 and the volume (L) of water habitats wanted in each spatial unit with the argument `lhvw`
258 (larval-habitat water volume, parameterised from Hancock et al. 2016; default `lhvw=2`;
259 see Fig S13 for a sensitivity analysis of this parameter). Moreover, the argument `temps.matrix`
260 takes the matrix of daily average temperature (in Celsius degree) used to fit the life cycle
261 rates. This matrix must be organised with the daily temperature observations as columns
262 and the geographic position of the *i*-grid cell as rows (it follows that the matrix will have
263 only one row when `scale="ws"`). The day of start, end and number of iterations are
264 defined by `startd`, `endd` and `iter`, respectively. The model has been optimised for
265 parallel computing and the number of parallel processes can be specified through the op-
266 tion `n.clusters`. If the modelled species is *Ae. albopictus*, *Ae. japonicus* or *Ae.*
267 *koreicus* (e.g., `species="albopictus"`) then the arguments defining latitude (`lat`),
268 longitude (`long`) and year of introduction (`intro.year`) should be adequately defined
269 to allow a correct switch to and from the egg diapausing stage.

270 The default output of `dynamAedes` consists of a list of numerical matrices containing,
271 for each iteration, the number of individuals in each life stage per day (and for each grid
272 cell of the study area if `scale="lc"` or `"rg"`). If the argument `compressed.output=FALSE`
273 (default `TRUE`), the model returns the daily number of individuals in each life stage sub-
274 compartment. The model, coded in the R statistical language (R Core Team, 2021),
275 and adapted for parallel computation, is available on the the following link [https:](https://github.com/mattmar/dynamAedes)
276 [//github.com/mattmar/dynamAedes](https://github.com/mattmar/dynamAedes) (it has meanwhile been submitted to the
277 [CRAN](#)).

```
#model parameters 1
cl=47 #number of cluster 3
it=100 #number of iterations 3
ie=500 #number of introduced eggs 5
str=1 #day intro 5
endr=ncol(wwl) #day end simulations 7

aeg.cal <- dynamAedes(species="aegypti", 9
                      scale="rg", 9
                      temps.matrix=wwl, 11
                      startd=str, endd=endr, 11
                      n.clusters=cl, 13
                      iter=it, 13
                      intro.eggs=ie, 15
                      ihwv=100, 15
                      verbose=FALSE) 17

albo.cal <- dynamAedes(species="albopictus", 19
                       lat=37, long=-120, 19
                       intro.year=2015, 21
                       scale="rg", 21
                       temps.matrix=wwl, 23
                       startd=str, endd=endr, 23
                       n.clusters=cl, 25
                       iter=it, 25
                       intro.eggs=ie, 27
                       ihwv=100, 27
                       verbose=FALSE)
```

278

279 2.3.1 Spatial scales of the model and input temperature data

280 The selection of the geographical scale for population dynamics is a crucial aspect of
281 the whole package and the temperature dataset provided to `dynamAedes` function must
282 reflect this decision. Along with the photoperiod, temperature is the other only environ-
283 mental driver of our model, which is dictated by its central role in mosquito develop-
284 ment and activity. The measurement of temperature is inevitably scale-dependent, thus we
285 structured the model to allow for temperature datasets relevant for different measurement
286 spatial scales (Fig. 2) and to match the different hypotheses that users may want to test.

287 The punctual or "weather station" scale (`scale="ws"`) is the smallest geographic
288 scale (i.g., no spatial dimension) available in `dynamAedes` and the environment mod-

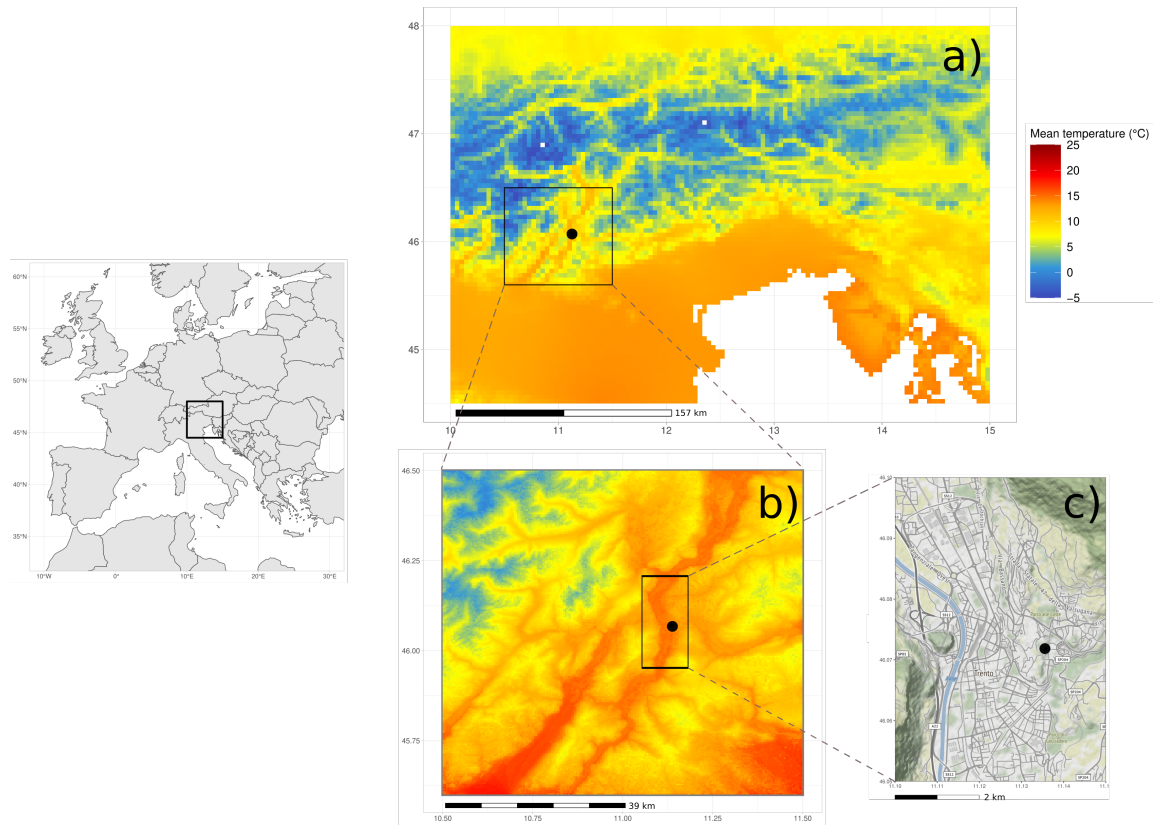


Figure 2: dynamAedes allows to simulate *Aedes* mosquitoes population dynamics at three different spatial scales: a) regional, b) local, and c) punctual (weather station). Passive and active dispersal is enabled only at local spatial scale.

289 elled is assumed to be what represented by the chosen weather station (or any other data-
290 loggers). In this case, the model has no spatial structure, thus dispersal is not considered:
291 the model will return the temporal trend of population dynamics given the chosen temper-
292 ature, larval-habitat water volume and photoperiod conditions.

293 The "local" scale (`scale= "lc"`) represents those scenarios and spatial resolutions
294 at which species dispersal and local microclimate variability are relevant for users. We
295 suggest to keep the resolution of the matrix of temperatures equal or smaller than the
296 maximum daily dispersal range of the mosquito species (i.e., usually under 1 km for
297 *Aedes* species; Guerra et al., 2014). The optional arguments `cellsize`, `dispbins`
298 and `maxdisp` are available to fine tune the dispersal kernel which drives the spatial
299 behaviour of the simulated mosquito populations. The argument `cellsize` (default
300 "`cellsize=250`" meters) sets the minimal distance of the dispersal kernel and should

301 match the size of the cell to avoid inconsistencies (i.e., mosquitoes dispersing at a finer
302 or bigger grain than the arena), `maxdisp` sets the maximum daily dispersal (default
303 `maxdisp=600` meters), and `dispbins` the resolution of the dispersal kernel (de-
304 fault `dispbins=10`). Passive dispersal is also implemented and it requires i) a matrix
305 containing the coordinates of the grid cells of the landscape intersecting the road network
306 (argument `road.dist.matrix`), and ii) to specify the average car trip distance through
307 the argument `country`, which can be defined by the user or considering estimates for
308 the following countries: France, Germany, Italy, Poland, Spain and the United Kingdom
309 Pasaoglu et al. (2012). An extensive example of model application at local spatial scales
310 is described in Da Re et al. (2021).

311 The rationale behind the third spatial scale considered in the model, the "regional"
312 scale (`scale= "rg"`) was to return an overview of invasive *Aedes* population dynamics
313 over large extents (i.e., larger than 1 km). The model in regional scale does not account
314 for species dispersal, introductions happen separately (but at the same time) in each grid
315 cell which hence are closed systems. The output of the model at "regional" scale can be
316 compared to those produced by correlative species distribution models (SDMs), with the
317 advantage of mechanistic rather than purely correlative model foundations.

318 The amount of water available for larval development in each spatial unit(s) (at any
319 model spatial scale) was set as 2 L that is the water volume considered in the experiments
320 we used to parametrise model functions Hancock et al. (2016). It is likely that for many
321 real-world model applications, the relative availability of breeding habitats is much higher,
322 and we encourage users to set a value based on their scenarios and hypotheses (i.e. through
323 the model option `lhvw`; Hartemink et al. 2015).

324 **2.3.2 Auxiliary functions**

325 Several auxiliary functions are available to analyse model outputs. The function `psi` re-
326 turns the proportion of model iterations that resulted in a viable population for the given
327 date. It works for all spatial scales and the output can reflect either the overall grid or
328 each single cell. Likewise, summaries of mosquito abundance at each life stage for each
329 day can be obtained through `adci`, which by default returns the inter-quartile range abun-
330 dance of each life stage. Similarly, `icci` returns a summary of the number of invaded cells
331 over model iterations. Estimates of dispersal spread (in km²) of the simulated mosquito
332 populations is provided by the function `dici`, which is available only for model results
333 computed at the local scale (the only scale which integrates dispersal). Finally, the function
334 `get_rates_spatial`, returns the output of the temperature-dependent physiological
335 functions used by `dynamAedes` to derive the daily rates. It can be used to better under-
336 stand the outcome of model simulations, by highlighting those areas where the predicted

337 values of the temperature-dependent functions are maximised or minimised, or to derive
338 causal-based physiological estimations that, for example, could be used as inputs for cor-
339 relative SDMs (e.g., Kearney and Porter, 2009; Mathewson et al., 2017).

340 **3 Case studies and model validation**

341 We applied the model to three case studies representing different geographical scales and
342 areas, species and invasion trajectories. The case studies were chosen considering the
343 availability of optimal mosquito data-sets to show model strength and weakness. We did
344 not report any example for the "local scale" as it had already been provided in Da Re et al.
345 (2021), who applied a previous version of `dynamAedes`.

346 **3.1 Regional scale models**

347 **3.1.1 Likelihood of successful introductions of *Ae. albopictus* and *Ae. aegypti* across** 348 **California, USA**

349 We used `dynamAedes` at "regional" scale to assess the likelihood of successful intro-
350 ductions for two invasive *Aedes* across California: *Ae. aegypti* and *Ae. albopictus* which
351 are considered established from 2011 and 2013, respectively (Fujioka, 2012; Gloria-Soria
352 et al., 2014). California is among the few areas where established populations of these two
353 species were detected during the last decade and their progressive spread was documented
354 in great detail². We downloaded daily minimum and maximum temperature data from the
355 NASA Daily Surface Weather Data on a 1-km Grid for North America (DAYMET), Ver-
356 sion 4 (Thornton et al., 2020) from 1 January 2011 to the 31 December 2018. These two
357 sets of data (in netCDF raster format) were clipped to the boundary of California and ag-
358 gregated at a spatial resolution of 2.5 km by using a combination of GDAL (GDAL/OGR
359 contributors, 2021) and Climate Data Operators (CDO; Schulzweida, 2019) software. The
360 two sets of raster layers were then imported in R 4.0.4 (R Core Team, 2021), transformed
361 in matrices, averaged and converted to integers to obtain a single average daily temper-
362 ature integer matrix with cell id as observations (rows) and days as variables (columns).
363 This dataset was used as the input temperature matrix for the model. We run 80 model
364 iterations for five years, introducing 500 eggs in each cell of the gridded landscape on 15
365 May 2011 and 2013 for *Ae. aegypti* and *Ae. albopictus* respectively. By using the auxil-
366 iary function `psi`, we then derived a map showing the proportion of iterations with viable
367 population of both *Ae. aegypti* and *Ae. albopictus* at the end of the simulated period (15

²See <https://maps.vectorsurv.org/>

368 May 2016 and 2018). The photoperiod was set to match conditions in the geographical
369 center of California (Lat 37° N, Lo -120° W) and the amount of breeding habitat was set
370 to 100 L (per cell), which we assumed to be representative of the potential water larval
371 habitats available given cell size and overall regional climate.

372 We validated model prediction using maps of cities in California with known species
373 presence updated to 2021 by the California Department of Public Health (CDPH³). We
374 derived the average predicted probability of successful introduction for each city and com-
375 puted the Area Under the ROC Curve (AUC) score which defines the probability that a
376 randomly chosen positive city will be ranked higher than a randomly chosen negative city.
377 An AUC score > 0.5 indicates that the model is performing better than random, while a
378 score of 1 indicates perfect prediction. In addition, we calculated the percentage of posi-
379 tive cities that fell into a grid cell that had a probability of establishment higher or equal to
380 1% (e.g., at least 1 out of the n_{th} iterations reported a viable mosquito population in that
381 cell).

382 The predicted spatial pattern of areas with a high likelihood of *Ae. aegypti* and *Ae.*
383 *albopictus* successful introduction is in general consistent with updated information on
384 the presence of this species (Fig. 3). Predictions show moderate-to-high probabilities of a
385 successful introduction in all counties with known presence of these species, except for the
386 extreme South-East coastal part of the state, where *Ae. aegypti* was predicted to have a low
387 probability of successful introduction whereas being well established (Fig. 3). This may
388 be due to the high micro-climatic variability that characterises coastal areas of California
389 which may not be resolved by the temperature datasets that we have considered in this case
390 study. On the contrary, areas predicted to be suitable for *Ae. albopictus* exceeded by far the
391 known current distribution of this species. Factors other than temperature and photoperiod,
392 more nuanced aspects of species invasion history and the extremely low humidity during
393 the dry season in the Central Valley of California or the Inland Empire, may hinder species
394 establishment in these areas. Nevertheless, recently *Ae. albopictus* was found as north as
395 Redding, Shasta County, thus it is not unlikely that this species is also present (perhaps at
396 low densities), but not yet detected, at southern latitudes in California.

397 Both models had over 75% of successful introduction scores (calculated as the pro-
398 portion of pixels with species observations and simulated proportion of invasion > 1%)
399 when validated at city levels (Tab. 1). Still, only the prediction for *Ae. aegypti* validated at
400 city levels reported an AUC score bigger than 0.5 (Tab. 1), whereas validating the model
401 by averaging the predictions at county level resulted in an AUC bigger than 0.5 for both
402 species (0.892 and 0.717 for *Ae. aegypti* and *Ae. albopictus* respectively; Fig. S14).

³California Department of Public Health, "Map and City List of *Aedes aegypti* and *Aedes albopictus* Mosquitoes in CA, 2011-2021" (accessed on 28th October 2021): <https://www.cdph.ca.gov/Programs/CID/DCDC/Pages/VBDS.aspx>

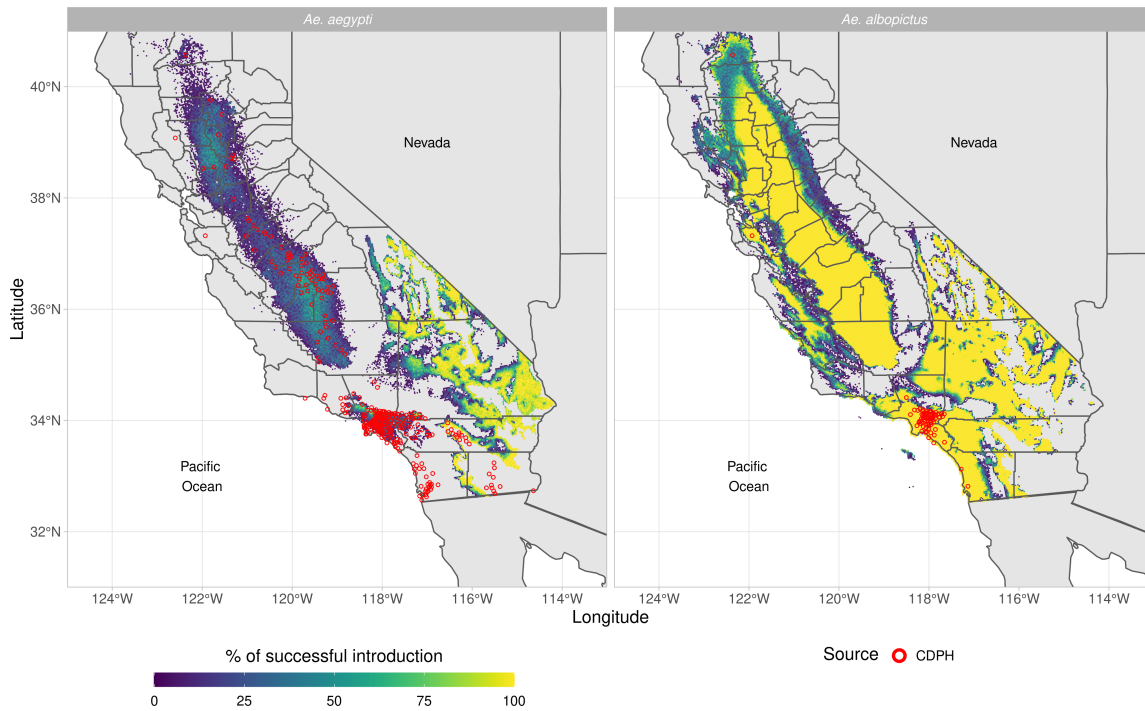


Figure 3: Predicted percentage of established introductions of *Ae. aegypti* *Ae. albopictus* in California (USA) for the years 2011-2016 and 2013-2018, respectively. The red dots represent the centroids of the Californian municipalities with established populations as reported by the Californian Department of Public Health (CDPH).

403 3.1.2 Likelihood of successful *Aedes albopictus* introductions in France

404 *Aedes albopictus* was first detected in metropolitan France in 1999 (Schaffner et al., 2000)
405 and since 2004 it has established populations in the southern part of the country while
406 still expanding its distribution range (ECDC, 2021). We used *dynamAedes* model at
407 "regional" scale to assess the success of introductions of *Ae. albopictus* for the whole
408 metropolitan France. We processed ERA5-Land (Muñoz-Sabater et al., 2021) hourly air
409 temperature measured at 2 m above surface from January 1st 2015 to December 31st 2020
410 in the Climate Data Store (CDS) Toolbox⁴ to get the daily mean temperature of the period
411 considered for the whole metropolitan France, at the spatial resolution of ~ 9 km. The
412 netCDF file obtained was imported in R 4.0.4 (R Core Team, 2021), where was clipped
413 to the extent of metropolitan France, converted from degrees Kelvin to Celsius and con-
414 verted to integer to obtain a single average daily temperature integer matrix with cell id

⁴CDS Toolbox: <https://cds.climate.copernicus.eu/toolbox/doc/index.html>

415 as observations (rows) and days as variables (columns). This dataset was then used as the
416 input temperature matrix for the model. We run 100 simulations for five years, introducing
417 100 eggs in each cell of the gridded landscape on 15 May 2015. By using the auxiliary
418 function `psi`, we derived a probability map of the areas showing the proportions of iter-
419 ations that produced a viable population of *Ae. albopictus* five years after the simulated
420 introductions.

421 We validate the model predictions using the list of the 3419 French municipality re-
422 porting established *Ae. albopictus* until 2020 provided by the French Health Ministry (data
423 collected thanks to active monitoring from French mosquito operators and passive surveil-
424 lance⁵). Similarly to the previous case study, we computed both the AUC as well as the
425 proportion of positive location falling into a grid cell that had a percentage of established
426 introductions higher than or equal to 1%. The spatial pattern of the areas predicted to have
427 a high likelihood of successful *Ae. albopictus* introduction (Fig. 4) is consistent with up-
428 dated observational data (*Ae. albopictus* map; ECDC, 2020) as well as with the results of
429 other mechanistic models (see for instance Metelmann et al., 2019; Pasquali et al., 2020).
430 The Mediterranean French coast and the Rhone valley are the areas where our model pre-
431 dicted the highest percentage of successful introduction. Similarly, the Aquitaine region on
432 the Atlantic coast and the Alsace region in the North-East part of France showed relatively
433 high predicted percentage of successful introduction. The northern and the central part of
434 France, as well as the Pyrenees areas, show low percentage of successful introduction un-
435 der the current climatic conditions. However, the resolution of the pixel, approximately 10
436 km, may have played a role influencing the model outcomes especially in topographically
437 complex areas such as the Pyrenees or the French Alps, where the microclimate of the
438 valleys may be underestimated. Similarly, the model was not able to predict the successful
439 introduction of the species in areas such as Paris, where *Ae. albopictus* is established and
440 probably favoured by i) local climatic factors such as the urban heat island effect, and ii)
441 the continuous inflow of *Ae. albopictus* propagules to Paris from areas where the species
442 is already established. Indeed, most railways, flights and highways have a connection with
443 Paris, and the Paris-Lyon-Mediterranée axis is the main artery of France, with an average
444 of >60,000 cars/day on the highway⁶ and 240 trains per day⁷, thus the quantity of imported
445 mosquitoes can compensate for the less favorable climatic conditions of Paris compared
446 to the Mediterranean region (recent phylogeographic findings support this hypothesis, see
447 Sherpa et al., 2019). All the model performances metrics assessed support the capacity of
448 the model to discriminate between areas where the species can or cannot be established

⁵https://signalement-moustique.anses.fr/signalement_albopictus/

⁶<https://www.data.gouv.fr/fr/datasets/trafic-moyen-journalier-annuel-sur-le-reseau-r>

⁷<https://www.leparisien.fr/economie/l-europe-fait-passer-la-lgv-paris-lyon-a-l-heure>
php

449 (Tab. 1).

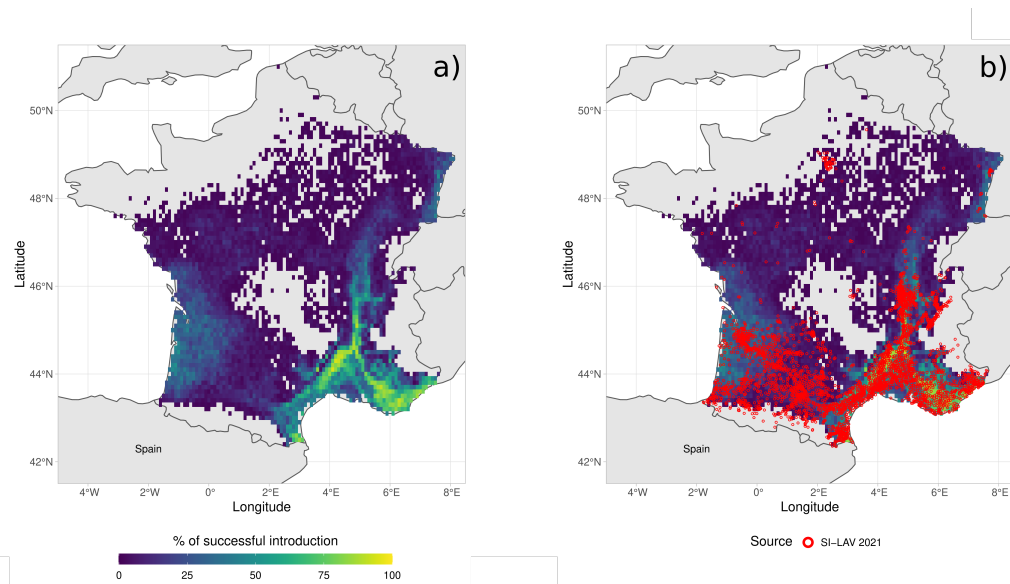


Figure 4: Percentage of successful introduction for *Ae. albopictus* in France for the years 2015-2020: a) Model prediction, b) Model prediction and in red the centroids of the French Municipalities with established population of *Ae. albopictus* reported by the French Health Ministry (SI-LAV).

450 **3.2 Punctual population dynamics temporal trends**

451 **3.2.1 *Aedes albopictus* population dynamics in Nice, South-East France**

452 *Aedes albopictus* is established mainly in the southern part of metropolitan France where
453 more than 40% of municipalities are colonized⁸ and it is still expanding in other areas. We
454 computed the population dynamics of the species informing dynamAedes model at punct-
455 tual spatial scale using temperature observations downloaded from the National Oceanic
456 and Atmospheric Administration (NOAA) network via the R package rnoaa. The obser-
457 vations of the NOAA weather station located in Nice area (usaf code = 076900, Lat 43°
458 42' 00" N, Lon 7° 13' 12" E, 3.7 m a.s.l.), spanning from January 1st 2013 to December
459 31st 2018, were linearly interpolated to fill missing values at hourly and daily level. Af-
460 terwards, the daily average for all observations was computed. We run 100 simulations
461 for five years, introducing 500 eggs on 15 May 2013. By using the auxiliary function
462 adci, we then derived the daily abundance inter-quantile range for each life stage and the
463 abundance of newly-laid eggs per day.

464 The model was validated comparing the simulated newly laid eggs per day to egg
465 counts from mosquito ovitrap data, following the validation approach presented in Tran
466 et al. (2013). During the years 2014-2018, fifty ovitraps were installed in the Nice area and
467 inspected fortnightly from April-May to November-December (data collected and kindly
468 provided by EID Méditerranée). We computed the Spearman's *rho* correlation coefficient
469 between the weekly-aggregated simulated newly-laid eggs and the mean observed eggs
470 per day.

471 Results showed that the model was able to correctly reproduce the seasonal dynamics
472 of the new-laid eggs over five years (Spearman's *rho* = 0.753, p.value < 0.001). The first
473 simulated eggs were laid during the late spring each year, confirming the fact that the first
474 overwintering eggs hatch at the end of the winter season or at the beginning of spring.
475 The ovipositing season seem to last until the late autumn accordingly to the observations,
476 while our model seems to predict a shorter length of the ovipositing period. Nevertheless
477 the model is able to correctly infer the peak of the ovipositing season during the summer
478 months (Fig. 5).

479 **3.2.2 *Aedes koreicus* population dynamics in Trento, North-East Italy**

480 *Aedes koreicus* was first detected in Trento Autonomous Province (NE Italy) in 2013, soon
481 after the first Italian detection in the neighboring Belluno province (Capelli et al., 2011).

⁸<https://solidarites-sante.gouv.fr/sante-et-environnement/risques-microbiologiques-physiques-et-chimiques/especes-nuisibles-et-parasites/article/cartes-de-presence-du-moustique-tigre-aedes-albopictus-en-france-metropolitain>

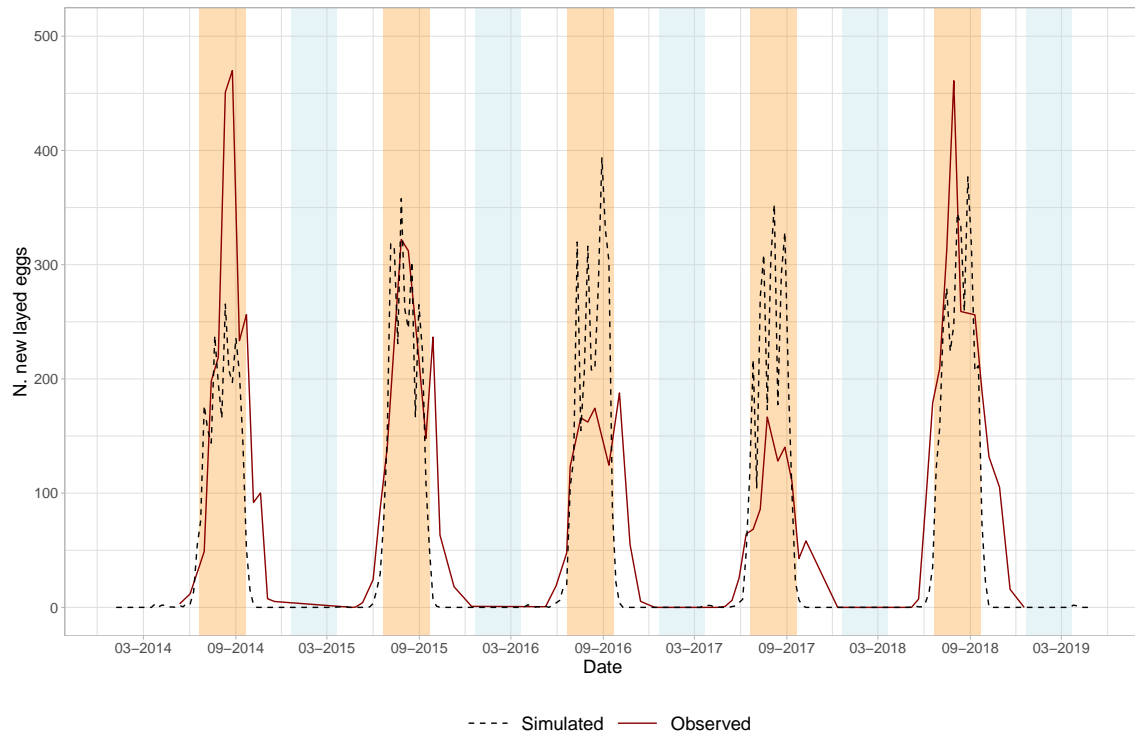


Figure 5: Temporal trend reporting the simulated and observed new-laid eggs of *Ae. albopictus* years 2014-2018 in Nice, SE France. The light blue bands represent the winter seasons, while the orange bands the summer seasons. The simulated data were rescaled for graphical purpose using as rescaling factor the ratio between the maximum observed value and the maximum median simulated values.

482 We computed the population dynamics of the species informing `dynamAedes` model
483 at punctual spatial scale using temperature observations downloaded from the local net-
484 work of weather stations⁹. The daily average temperature observations from the "Trento
485 Laste" weather station (Lat 46° 04' 18.5" N, Lon 11° 08' 08.5" E, 312 m a.s.l.) spanning
486 from 1 January 2015 to 31 December 2018 were linearly interpolated to fill missing val-
487 ues. We run 100 simulations for five years, introducing 500 eggs on 15 May 2015. Using
488 the auxiliary function `adci`, we then derived the daily inter-quartile range abundance for
489 each life stage and for the daily host-seeking female sub-compartment.

490 The model was validated computing Spearman's *rho* correlation coefficient between
491 the monthly-aggregated simulated host-seeking females and the observations gathered

⁹www.meteotrentino.it

492 from four BG-Sentinel traps installed in Trento municipality from April to November dur-
493 ing the years 2016, 2017, and 2018 (data obtained from Marini et al. 2019b). In order
494 to compare observed and simulated data, the whole simulated host-seeking females abun-
495 dance was multiplied by a BG-sentinel catching rate equal to 0.157, as estimated by Marini
496 et al. (2019b) and similar to what already reported for *Ae. albopictus* in previous studies
497 (Guzzetta et al., 2017).

498 The simulated population dynamics showed that *Ae. koreicus* could be successfully
499 introduced in the study area. The model correctly predicted the start of the seasonal ac-
500 tivity in early spring, while the higher abundance of female host-seeking mosquitoes was
501 predicted to be in late summer. Considering the three years together, our model was able
502 to reproduce the observed seasonal population dynamics, where the 76.2% (47.6%) of the
503 observed captures lie within the 95% (50%) credible intervals of model predictions (Tab
504 S7). Similarly, the Spearman's rho for the three years was 0.735 (p.value < 0.001) (Tab. 1)

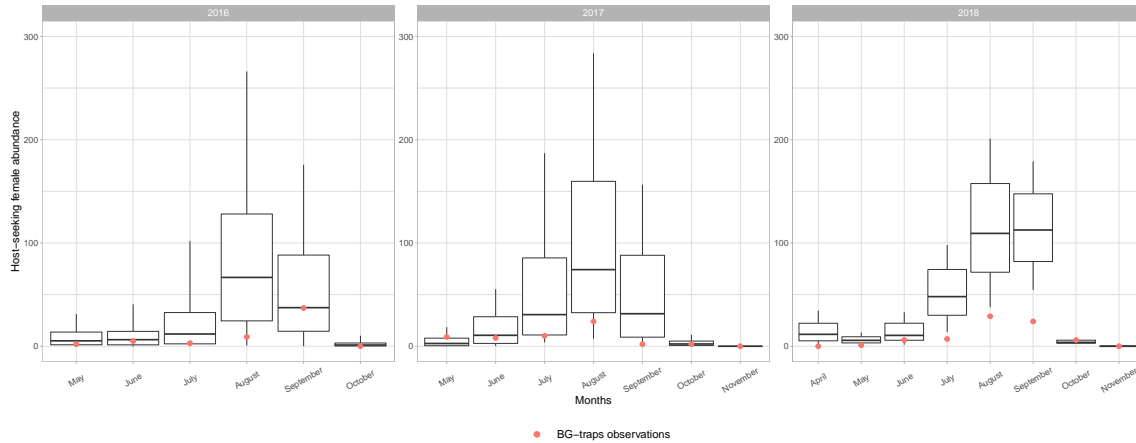


Figure 6: Temporal trend reporting the boxplot of simulated and observed host-seeking *Ae. koreicus* females for the years 2016-2018 in Trento, NE Italy.

Species	Geographic location	Scale	AUC	Specificity	Sensitivity	Sensitivity 1%	Spearman's ρ
<i>Ae. aegypti</i>	California	Regional	0.658 (0.401-0.914)	0.8	0.642	0.795	-
<i>Ae. albopictus</i>	California	Regional	0.435 (0.367-0.502)	0.241	0.641	1	-
<i>Ae. albopictus</i>	France	Regional	0.874 (0.867-0.880)	0.788	0.802	0.848	-
<i>Ae. albopictus</i>	S-E France	Punctual	-	-	-	-	0.753***
<i>Ae. koreicus</i>	N-E Italy	Punctual	-	-	-	-	0.735***

Table 1: Model validation. The column "Sensitivity 1%" reports the proportion of cities predicted to have at least one successful introduction over the total number of iterations (predicted introduction success equal or over 1%. *** p.value < 0.001).

505 4 Discussion

506 From an ecological perspective, our modelling approach focuses on the species funda-
507 mental thermal niche (*sensu* Hutchinson, 1957), since we considered temperature as the
508 main driver of population growth and dynamics. In light of this, our model was able to in-
509 fer spatial and temporal population dynamics of different species, at different geographic
510 scales and locations. The model showed overall good validation performance, and the ar-
511 eas predicted to likely support *Aedes* mosquito populations largely matched what reported
512 by observational studies and other existing models (Kraemer et al., 2015, 2019; Oliveira
513 et al., 2021).

514 Nevertheless, we raise the attention on two aspects that should be considered when
515 applying `dynamAedes` and interpreting model results. First, good quality information on
516 survival and developmental rates is largely available for *Ae. aegypti* and *Ae. albopictus*,
517 whereas much less for the other two species. Similarly, mosquito observational datasets
518 with sufficient longitudinal depth for model validation are scarce for *Ae. koreicus* and
519 presently absent, to the best of our knowledge, for *Ae. japonicus*. Thus, whilst we have
520 built the foundations for an open-source modelling framework that can be progressively
521 expanded, life cycle functions and thus outputs for *Ae. japonicus* and *Ae. koreicus* should
522 be interpreted more carefully.

523 Secondly, we recognise that pixel size may influence model outcome because of the
524 aggregating effect of the Modifiable Unit Areal Problem (Jelinski and Wu, 1996; Da Re
525 et al., 2020). While the consequences of this artifact are well known in SDMs applications,
526 they are rarely mentioned or addressed (but see Peterson, 2014). Thus, the correct choice
527 of temperature datasets is crucial to investigate species population dynamics and interpret
528 model results (Bütikofer et al., 2020). Climatic reanalysis and Global/Regional Circula-
529 tion Models are reliable data sources with high temporal resolution for present climatic
530 conditions and robust future projections, though they have a coarse spatial resolution that
531 may underestimate the effect of microclimate on species biology (Metelmann et al., 2019;

532 Liu-Helmersson et al., 2019). Coarse resolution of input temperature data is rather com-
533 mon since temperature is often estimated over large extents, and can become an issue in
534 topographically complex regions where the effect of microclimatic variation on population
535 dynamics may pass undetected. The results showed in Fig. 3–4 may be better interpreted
536 considering the coarse resolution of temperature data which may have caused lower pro-
537 portion of established populations in topographically complex areas such as the Pyrenees
538 or the Peninsular Ranges. Interpolated local micro-climatic conditions, for example esti-
539 mated with the `microclima` R package (Maclean et al., 2019), have the advantage of
540 providing fine spatial and temporal resolution datasets. But, they need to be first properly
541 validated with field data which are typically difficult to gather also over small geograph-
542 ical extents. Temperature measured with classical weather stations may be considered as
543 the most accurate available observations of local climatic conditions. Though it is not al-
544 ways easy to deal with such data due to the limited number of weather stations and gaps
545 in the time series, they are suited for statistical downscaling or bias adjustment for climate
546 change projections (Bedia et al., 2020).

547 **4.1 Model assumptions**

548 Model structure has been designed to be as ecologically relevant as possible considering
549 available data, however, when data were limited, we relied on a set of "expert-based"
550 assumptions that must be clearly stated.

551 The interplay of multiple environmental factors drives the population dynamics of
552 *Aedes* mosquitoes but we chose to mold our model framework just on established infor-
553 mation available for temperature and photo-period (Pumpuni et al., 1992; Waldoek et al.,
554 2013; Eisen et al., 2014). This choice was suggested by a generalised lack of clear relation-
555 ships between other environmental factors and *Aedes* population dynamics. For example,
556 concerning the role of precipitations, different studies report contrasting results (Koen-
557 raadt and Harrington, 2008; Tran et al., 2013; Caldwell et al., 2021). Moreover, invasive
558 *Aedes* mosquitoes mostly thrive in urban or suburban landscapes where the presence of
559 standing water is often independent from precipitations (except for extreme rainfall events
560 (Roiz et al., 2015). We suggest that, at the present stage, `dynamAedes` it is better suited
561 for applications in temperate climates, where temperature seasonality is a more important
562 limiting factor than in tropical climates, where other factors may limit mosquito life cycle
563 Lega et al. (2017).

564 On the one hand, we did not consider in the model biotic interactions such as prey-
565 predator or food and space competition with other mosquito taxa during the larval stages,
566 despite this is another factor that influences the trajectory of introduced populations (Armis-
567 tead et al., 2008; Tripet et al., 2011; Reiskind and Lounibos, 2013; Montarsi et al., 2013,

568 2015b; Müller et al., 2018). On the other hand, we considered the effect of intra-specific
569 competition on larval survival (but not development). We generalised the information
570 available for *Ae. aegypti* to the other *Aedes* species due to the lack of species-specific ex-
571 periments (Hancock et al., 2016). We recognise that this is not optimal under many facets,
572 but intra-specific larval interactions were a key driver of mosquito-population dynamics
573 that could not be excluded by model structure.

574 Finally, we did not consider evolutionary processes in our model which may affect
575 invasion success over medium-long time spans. Given the reproductive strategy of *Aedes*
576 mosquitoes, rapid evolutionary processes may take place over relatively short temporal
577 periods (e.g. decades), making introduced populations able to extend their original niche
578 (McBride et al., 2014b).

579 **4.2 Proposed research directions**

580 `dynamAedes` is an open-source tool for testing ecological hypothesis and/or to support
581 management plans concerning AIMs. Selecting areas at risk of AIM establishment or pe-
582 riods when abundances are more likely to peak should be considered as facets of AIM
583 surveillance. The importance of such early information becomes fundamental for protect-
584 ing human health when treating AIM involved in pathogen transmission, as early informa-
585 tion on new trajectories of AIM populations becomes critical in the current climate change
586 era. Mosquitoes are affected by temperature changes in, often, predictable ways, though
587 changes in population dynamics can be extremely rapid. Modelling population dynamics
588 under climate change scenarios may thus provide information for anticipating both AIM
589 population changes in space and time and human health risks.

590 The conceptualisation and design of `dynamAedes` required the review of up-to-date
591 ecological and physiological literature available on four *Aedes* species, which was in-
592 tegrated with feedback from expert ecologists and medical entomologists. It emerged
593 that knowledge on some ecological aspects of these species is highly fragmented or poor
594 (e.g., Cebrián-Camisón et al. 2020), and often dependant on experimental settings and
595 lab strain (e.g., Kramer et al. 2020). Thus, the exploitation of such sets of information
596 for process-based models and, hence, for AIM management would greatly benefit from a
597 standardised review effort and possibly centralised repositories, as already done in other
598 scientific fields such as plant functional traits (Kattge et al., 2020) or systems biology
599 (Tsigkinopoulou et al., 2018). Moreover, experiments on *Ae. japonicus* and *Ae. koreicus*
600 life cycles are just starting to unravel these species eco-physiological rates (*Ae. koreicus*:
601 (Ciocchetta et al., 2017; Marini et al., 2019b); *Ae. japonicus*: (Scott, 2003; Reuss et al.,
602 2018; Wieser et al., 2019) and much work remain to be done on this species. On the con-
603 trary, there is large information concerning *Ae. aegypti* and *Ae. albopictus* physiological

604 rates which anyhow have been shown to be highly heterogeneous (Eisen et al., 2014) likely
605 due to non-standardised experimental designs and ecological plasticity of *Aedes* popula-
606 tions (*sensu* Kramer et al. 2021). Information regarding mosquito dispersal is even scarcer
607 and available only for *Ae. aegypti* and *Ae. albopictus*, while passive dispersal through
608 auto-vehicles has been estimated only for *Ae. albopictus* (Eritja et al., 2017) despite the
609 worldwide spread of *Aedes* species was most likely caused by means of passive dispersal.

610 From a biological perspective, future developments of `dynamAedes` may consider
611 also the addition of a `strain` argument, where the physiological temperature-dependent
612 function can be fitted on geographically different mosquito strains, such as tropical, mediter-
613 ranean or temperate (Marini et al., 2020; Kramer et al., 2021). Moreover, if observational
614 data are available, calibration of some parameters values, such as the juvenile density-
615 dependent mortality rate, might be implemented following for instance a Bayesian ap-
616 proach (Marini et al., 2019b).

617 We believe that a closer interaction between modelers and experimenters will mo-
618 tivate the collection of standardised data on unknown eco-physiological AIM rates that
619 would lead to more accurate model predictions. This project was inspired by such inter-
620 actions and, in this spirit, `dynamAedes` was meant to be modified or extended to relax
621 its assumptions and limitations with new available information by anyone having basic R
622 programming skills.

623 5 Conclusion

624 In this study, we presented `dynamAedes`, a mechanistic process-based model to infer
625 invasive *Aedes* mosquito spatio-temporal population dynamics. This first version of the
626 model showed to be often reliable in terms of both biological realism and statistical ac-
627 curacy. The open-source nature and programming language accessibility and flexibility
628 of the project offers great potential to further develop the model, allowing to better tune
629 the temperature-dependent functions when new physiological observations and findings
630 become available. Abundance estimations derived from `dynamAedes` could be used to
631 inform epidemiological models (e.g., SIR or SEIR) and thus obtain estimations on the risk
632 of pathogens transmission. Finally, it does not seem unrealistic to extend the model appli-
633 cation to other species of the genus *Aedes* such as *Ae. notoscriptus* or to species belonging
634 to other genus of medical interest belonging to the *Culicidae* family, such as *Anopheles*,
635 or even to other blood-sucking insects belonging to different taxa such as *Culicoides*.

636 **6 Acknowledgements**

637 No conflict of interest has been declared by the author(s).

638 We thank the French Ministry of Health for providing the confirmed *Ae. albopictus*
639 established population data (SI-LAV), and the EID Méditerranée for providing us the
640 ovitraps data from Nice. Computational resources have been provided by the DART re-
641 search group at the University of California, Davis as well as supercomputing facilities of
642 the Université catholique de Louvain (CISM/UCL) and the Consortium des Équipements
643 de Calcul Intensif en Fédération Wallonie Bruxelles (CÉCI) funded by the Fond de la
644 Recherche Scientifique de Belgique (F.R.S.-FNRS) under convention 2.5020.11 and by
645 the Walloon Region.

646 DDR and MM are supported by the FRS-FNRS. MM is also supported by the “Ac-
647 tion de Recherche concertée” grant number 17/22-086. FR and RM were supported by the
648 Hessian Centre on Climate Change (FZK) of the Hessian Agency for Nature Conservation,
649 Environment and Geology (HLNUG). Research of RM was funded through the 2018-2019
650 BiodivERsA joint call for research proposals, under the BiodivERsA3 ERA-Net COFUND
651 programme, and with the funding organisation FWO (BiodivERsA2018-A-323). The Out-
652 break Research Team of the Institute of Tropical Medicine is financially supported by the
653 Department of Economy, Science and Innovation of the Flemish government.

654 This project was done within the framework of AIM-COST Action CA17108 (www.aedescost.eu).
655

656 **7 Authors contribution**

657 MM and DDR conceived the ideas, designed the methodology and analysed the data;
658 WVB, FR, RM, SB, FM, SC, DA, GM, AP, GLA, GL and CJMK provided expert opinion
659 on mosquito biology as well as observational datasets to validate the model; DDR, MM
660 and SOV led the writing of the manuscript. All authors contributed critically to the drafts
661 and gave final approval for publication.

662 **References**

- 663 Abbo, S. R., Visser, T. M., Wang, H., Göertz, G. P., Fros, J. J., Abma-Henkens, M. H.,
664 Geertsema, C., Vogels, C. B., Koopmans, M. P., Reusken, C. B., et al. (2020). The inva-
665 sive Asian bush mosquito *Aedes japonicus* found in the Netherlands can experimentally
666 transmit Zika virus and Usutu virus. *PLoS neglected tropical diseases*, 14(4):e0008217.
- 667 Andreeva, Y. V., Khrabrova, N. V., Alekseeva, S. S., Abylkassymova, G. M., Simakova,
668 A. V., and Sibataev, A. K. (2021). First record of the invasive mosquito species *Aedes*
669 *koreicus* (Diptera, Culicidae) in the Republic of Kazakhstan. *Parasite*, 28:52.
- 670 Armistead, J., Arias, J., Nishimura, N., and Lounibos, L. (2008). Interspecific larval com-
671 petition between *Aedes albopictus* and *Aedes japonicus* (Diptera: Culicidae) in Northern
672 Virginia. *Journal of medical entomology*, 45(4):629–637.
- 673 Baldacchino, F., Caputo, B., Chandre, F., Drago, A., della Torre, A., Montarsi, F., and
674 Rizzoli, A. (2015). Control methods against invasive *Aedes* mosquitoes in Europe: a
675 review. *Pest management science*, 71(11):1471–1485.
- 676 Barzon, L., Gobbi, F., Capelli, G., Montarsi, F., Martini, S., Riccetti, S., Sinigaglia, A.,
677 Pacenti, M., Pavan, G., Rattu, M., et al. (2021). Autochthonous dengue outbreak in
678 Italy 2020: clinical, virological and entomological findings. *Journal of travel medicine*.
- 679 Bedia, J., Baño-Medina, J., Legasa, M. N., Iturbide, M., Manzananas, R., Herrera, S.,
680 Casanueva, A., San-Martín, D., Cofiño, A. S., and Gutiérrez, J. M. (2020). Statisti-
681 cal downscaling with the downscaler package (v3. 1.0): contribution to the VALUE
682 intercomparison experiment. *Geoscientific Model Development*, 13(3):1711–1735.
- 683 Brady, O. J. and Hay, S. I. (2019). The first local cases of Zika virus in Europe. *The*
684 *Lancet*, 394(10213):1991–1992.
- 685 Bütikofer, L., Anderson, K., Bebbber, D. P., Bennie, J. J., Early, R. I., and Maclean, I. M.
686 (2020). The problem of scale in predicting biological responses to climate. *Global*
687 *Change Biology*, 26(12):6657–6666.
- 688 Caldwell, J. M., LaBeaud, A. D., Lambin, E. F., Stewart-Ibarra, A. M., Ndenga, B. A.,
689 Mutuku, F. M., Krystosik, A. R., Ayala, E. B., Anyamba, A., Borbor-Cordova, M. J.,
690 et al. (2021). Climate predicts geographic and temporal variation in mosquito-borne
691 disease dynamics on two continents. *Nature communications*, 12(1):1–13.

- 692 Capelli, G., Drago, A., Martini, S., Montarsi, F., Soppelsa, M., Delai, N., Ravagnan, S.,
693 Mazzon, L., Schaffner, F., Mathis, A., et al. (2011). First report in Italy of the exotic
694 mosquito species *Aedes (Finlaya) koreicus*, a potential vector of arboviruses and filariae.
695 *Parasites & vectors*, 4(1):1–5.
- 696 Cebrián-Camisón, S., Martínez-de la Puente, J., and Figuerola, J. (2020). A literature
697 review of host feeding patterns of invasive *Aedes* mosquitoes in Europe. *Insects*,
698 11(12):848.
- 699 Christophers, S. R. (1960). *Aedes aegypti (L.) The Yellow Fever Mosquito: Its Life*
700 *History, Bionomics and Structure*. Cambridge University Press. Google-Books-ID:
701 TBcf5DTKL1oC.
- 702 Ciocchetta, S., Darbro, J. M., Frentiu, F. D., Montarsi, F., Capelli, G., Aaskov, J. G., and
703 Devine, G. J. (2017). Laboratory colonization of the European invasive mosquito *Aedes*
704 (*Finlaya*) *koreicus*. *Parasites & vectors*, 10(1):1–6.
- 705 Ciocchetta, S., Prow, N. A., Darbro, J. M., Frentiu, F. D., Savino, S., Montarsi, F., Capelli,
706 G., Aaskov, J. G., and Devine, G. J. (2018). The new European invader *Aedes (Fin-*
707 *laya) koreicus*: a potential vector of chikungunya virus. *Pathogens and Global Health*,
708 112(3):107–114.
- 709 Da Re, D., Gilbert, M., Chaiban, C., Bourguignon, P., Thanapongtharm, W., Robinson,
710 T. P., and Vanwambeke, S. O. (2020). Downscaling livestock census data using mul-
711 tivariate predictive models: Sensitivity to modifiable areal unit problem. *PloS one*,
712 15(1):e0221070.
- 713 Da Re, D., Montecino-Latorre, D., Vanwambeke, S. O., and Marcantonio, M. (2021). Will
714 the yellow fever mosquito colonise Europe? Assessing the re-introduction of *Aedes*
715 *aegypti* using a process-based population dynamical model. *Ecological Informatics*,
716 61:101180.
- 717 da Silva Neves, N. A., da Silva Ferreira, R., Morais, D. O., Pavon, J. A. R., de Pinho, J. B.,
718 and Shhessarenko, R. D. (2021). Chikungunya, Zika, Mayaro, and Equine encephalitis
719 virus detection in adult *Culicinae* from South Central Mato Grosso, Brazil, during the
720 rainy season of 2018. *Brazilian Journal of Microbiology*, pages 1–8.
- 721 Day, C. A., Lewandowski, K., Vonesh, J. R., and Byrd, B. D. (2020). Phenology of
722 rock pool mosquitoes in the southern Appalachian mountains: Surveys reveal apparent
723 winter hatching of *Aedes japonicus* and the potential for asymmetrical stage-specific
724 interactions. *Journal of the American Mosquito Control Association*, 36(4):216–226.

- 725 De Carlo, C. H., Campbell, S. R., Bigler, L. L., and Mohammed, H. O. (2020). *Aedes*
726 *japonicus* and West Nile Virus in new york. *Journal of the American Mosquito Control*
727 *Association*, 36(4):261–263.
- 728 Delatte, H., Paupy, C., Dehecq, J., Thiria, J., Failloux, A., and Fontenille, D. (2008). *Aedes*
729 *albopictus* , vecteur des virus du chikungunya et de la dengue à la Réunion : biologie et
730 contrôle. *Parasite*, 15(1):3–13.
- 731 Dzul-Manzanilla, F., Ibarra-López, J., Bibiano Marín, W., Martini-Jaimes, A., Leyva,
732 J. T., Correa-Morales, F., Huerta, H., Manrique-Saide, P., and Vazquez-Prokopec, G. M.
733 (2017). Indoor Resting Behavior of *Aedes aegypti* (Diptera: Culicidae) in Acapulco,
734 Mexico. *Journal of Medical Entomology*, 54(2):501–504.
- 735 ECDC (2021). European Centre for Disease Prevention and Control and
736 European Food Safety Authority. mosquito maps [internet]. stockholm:
737 Ecdc; 2021. [https://ecdc.europa.eu/en/disease-vectors/
738 surveillance-and-disease-data/mosquito-maps](https://ecdc.europa.eu/en/disease-vectors/surveillance-and-disease-data/mosquito-maps). Accessed: 2021-12-
739 01.
- 740 Effler, P. V., Pang, L., Kitsutani, P., Vorndam, V., Nakata, M., Ayers, T., Elm, J., Tom, T.,
741 Reiter, P., Rigau-Perez, J. G., Hayes, J. M., Mills, K., Napier, M., Clark, G. G., Gubler,
742 D. J., and Hawaii Dengue Outbreak Investigation Team (2005). Dengue fever, Hawaii,
743 2001-2002. *Emerging Infectious Diseases*, 11(5):742–749.
- 744 Eisen, L., Monaghan, A. J., Lozano-Fuentes, S., Steinhoff, D. F., Hayden, M. H., and
745 Bieringer, P. E. (2014). The impact of temperature on the bionomics of *Aedes* (*Ste-*
746 *gomyia*) *aegypti* , with special reference to the cool geographic range margins. *Journal*
747 *of medical entomology*, 51(3):496–516.
- 748 Erguler, K. (2018). sPop: Age-structured discrete-time population dynamics model in C,
749 Python, and R. *F1000Research*, 7:1220.
- 750 Erguler, K., Chandra, N. L., Proestos, Y., Lelieveld, J., Christophides, G. K., and Parham,
751 P. E. (2017). A large-scale stochastic spatiotemporal model for *Aedes albopictus*-borne
752 chikungunya epidemiology. *PloS one*, 12(3):e0174293.
- 753 Erguler, K., Smith-Unna, S. E., Waldoock, J., Proestos, Y., Christophides, G. K., Lelieveld,
754 J., and Parham, P. E. (2016). Large-scale modelling of the environmentally-driven pop-
755 ulation dynamics of temperate *Aedes albopictus* (skuse). *PloS one*, 11(2):e0149282.
- 756 Eritja, R., Palmer, J. R., Roiz, D., Sanpera-Calbet, I., and Bartumeus, F. (2017). Direct
757 evidence of adult *Aedes albopictus* dispersal by car. *Scientific Reports*, 7(1):1–15.

- 758 Eritja, R., Ruiz-Arrondo, I., Delacour-Estrella, S., Schaffner, F., Álvarez-Chachero, J.,
759 Bengoa, M., Puig, M.-Á., Melero-Alcíbar, R., Oltra, A., and Bartumeus, F. (2019).
760 First detection of *Aedes japonicus* in Spain: an unexpected finding triggered by citizen
761 science. *Parasites & vectors*, 12(1):1–9.
- 762 Focks, D., Haile, D., Daniels, E., and Mount, G. (1993a). Dynamic life table model
763 for *Aedes aegypti* (Diptera: Culicidae): simulation results and validation. *Journal of*
764 *medical entomology*, 30(6):1018–1028.
- 765 Focks, D. A., Haile, D., Daniels, E., and Mount, G. A. (1993b). Dynamic life table model
766 for *Aedes aegypti* (Diptera: Culicidae): analysis of the literature and model develop-
767 ment. *Journal of medical entomology*, 30(6):1003–1017.
- 768 Fujioka, K. (2012). Discovery of *Aedes albopictus* (Skuse) in the city of El Monte and the
769 initial response. *Proc. Pap. Mosq. Vect. Control Assoc. Calif.*, 80:27–29.
- 770 GDAL/OGR contributors (2021). *GDAL/OGR Geospatial Data Abstraction software Li-*
771 *brary*. Open Source Geospatial Foundation.
- 772 Gilpin, M. E. and McClelland, G. A. (1979). Systems analysis of the yellow fever
773 mosquito *Aedes aegypti*. *Fortschritte Der Zoologie*, 25(2-3):355–388.
- 774 Giron, S., Franke, F., Decoppet, A., Cadiou, B., Travaglini, T., Thirion, L., Durand, G.,
775 Jeannin, C., L’ambert, G., Grard, G., et al. (2019). Vector-borne transmission of Zika
776 virus in Europe, southern France, August 2019. *Eurosurveillance*, 24(45):1900655.
- 777 Gloria-Soria, A., Brown, J. E., Kramer, V., Yoshimizu, M. H., and Powell, J. R. (2014).
778 Origin of the Dengue Fever mosquito, *Aedes aegypti*, in California. *PLOS Neglected*
779 *Tropical Diseases*, 8(7):e3029.
- 780 Gloria-Soria, A., Lima, A., Lovin, D. D., Cunningham, J. M., Severson, D. W., and Powell,
781 J. R. (2018). Origin of a High-Latitude Population of *Aedes aegypti* in Washington, DC.
782 *The American Journal of Tropical Medicine and Hygiene*, 98(2):445–452.
- 783 Gradoni, F., Bertola, M., Carlin, S., Accordi, S., Toniolo, F., Visentin, P., Patregnani, T.,
784 Adami, S., Terzo, L., Dal Pont, M., et al. (2021). Geographical data on the occurrence
785 and spreading of invasive *Aedes* mosquito species in Northeast Italy. *Data in Brief*,
786 36:107047.
- 787 Gratz, N. G. (2004). Critical review of the vector status of *Aedes albopictus*. *Medical and*
788 *veterinary entomology*, 18(3):215–227. 00498 PMID: 15347388.

- 789 Guerra, C. A., Reiner, R. C., Perkins, T. A., Lindsay, S. W., Midega, J. T., Brady, O. J.,
790 Barker, C. M., Reisen, W. K., Harrington, L. C., Takken, W., Kitron, U., Lloyd, A. L.,
791 Hay, S. I., Scott, T. W., and Smith, D. L. (2014). A global assembly of adult fe-
792 male mosquito mark-release-recapture data to inform the control of mosquito-borne
793 pathogens. *Parasites & Vectors*, 7:276.
- 794 Guzzetta, G., Trentini, F., Poletti, P., Baldacchino, F. A., Montarsi, F., Capelli, G., Rizzoli,
795 A., Rosà, R., Merler, S., and Melegaro, A. (2017). Effectiveness and economic as-
796 sessment of routine larviciding for prevention of chikungunya and dengue in temperate
797 urban settings in Europe. *PLoS neglected tropical diseases*, 11(9):e0005918.
- 798 Hancock, P. A., Linley-White, V., Callahan, A. G., Godfray, H. C. J., Hoffmann, A. A.,
799 and Ritchie, S. A. (2016). Density-dependent population dynamics in *Aedes aegypti*
800 slow the spread of wMel *Wolbachia*. *Journal of Applied Ecology*, 53(3):785–793.
- 801 Harrington, L. C., Edman, J. D., and Scott, T. W. (2001). Why do female *Aedes aegypti*
802 (Diptera: Culicidae) feed preferentially and frequently on human blood? *Journal of*
803 *Medical Entomology*, 38(3):411–422.
- 804 Hartemink, N., Vanwambeke, S. O., Purse, B. V., Gilbert, M., and Van Dyck, H. (2015).
805 Towards a resource-based habitat approach for spatial modelling of vector-borne disease
806 risks. *Biological Reviews*, 90(4):1151–1162.
- 807 Hawley, W. A. (1988). The biology of *Aedes albopictus*. *Journal of the American Mosquito*
808 *Control Association. Supplement*, 1:1–39.
- 809 Hawley, W. A., Pumpuni, C. B., Brady, R. H., and Craig, G. B. (1989). Overwintering
810 Survival of *Aedes albopictus* (Diptera: Culicidae) Eggs in Indiana. *Journal of Medical*
811 *Entomology*, 26(2):122–129.
- 812 Hopkins, M. C., Zink, S. D., Paulson, S. L., and Hawley, D. M. (2020). Influence of forest
813 disturbance on La Crosse virus risk in Southwestern Virginia. *Insects*, 11(1):28.
- 814 Horváth, C., Cazan, C. D., and Mihalca, A. D. (2021). Emergence of the invasive Asian
815 bush mosquito, *Aedes (Finlaya) japonicus japonicus*, in an urban area, Romania. *Para-*
816 *sites & vectors*, 14(1):1–7.
- 817 Hurk, A. F. v. d., McElroy, K., Pyke, A. T., McGee, C. E., Hall-Mendelin, S., Day, A.,
818 Ryan, P. A., Ritchie, S. A., Vanlandingham, D. L., and Higgs, S. (2011). Vector Com-
819 petence of Australian Mosquitoes for Yellow Fever Virus. *The American Journal of*
820 *Tropical Medicine and Hygiene*, 85(3):446–451. Publisher: The American Society of
821 Tropical Medicine and Hygiene.

- 822 Hutchinson, G. (1957). Concluding remarks cold spring harbor symposia on quantitative
823 biology, 22: 415–427. *GS SEARCH*.
- 824 Iwamura, T., Guzman-Holst, A., and Murray, K. A. (2020). Accelerating invasion po-
825 tential of disease vector *Aedes aegypti* under climate change. *Nature Communications*,
826 11(1):1–10.
- 827 Jansen, S., Heitmann, A., Lühken, R., Jöst, H., Helms, M., Vapalahti, O., Schmidt-
828 Chanasit, J., and Tannich, E. (2018). Experimental transmission of Zika virus by *Aedes*
829 *japonicus japonicus* from southwestern Germany. *Emerging microbes & infections*,
830 7(1):1–6.
- 831 Jelinski, D. E. and Wu, J. (1996). The modifiable areal unit problem and implications for
832 landscape ecology. *Landscape ecology*, 11(3):129–140.
- 833 Juliano, S. A. (2007). Population Dynamics. *Journal of the American Mosquito Control*
834 *Association*, 23(2 Suppl):265–275.
- 835 Juliano, S. A., O’Meara, G. F., Morrill, J. R., and Cutwa, M. M. (2002). Desiccation and
836 thermal tolerance of eggs and the coexistence of competing mosquitoes. *Oecologia*,
837 130(3):458–469.
- 838 Kattge, J., Bönisch, G., Díaz, S., Lavorel, S., Prentice, I. C., Leadley, P., Tautenhahn, S.,
839 Werner, G. D. A., Aakala, T., Abedi, M., and Acosta, A. T. R. (2020). TRY plant trait
840 database – enhanced coverage and open access. *Global Change Biology*, 26(1):119–
841 188.
- 842 Kaufman, M. G. and Fonseca, D. M. (2014). Invasion biology of *Aedes japonicus japoni-*
843 *cus* (Diptera: Culicidae). *Annual Review of Entomology*, 59:31–49.
- 844 Kearney, M. (2006). Habitat, environment and niche: what are we modelling? *Oikos*,
845 115(1):186–191.
- 846 Kearney, M. and Porter, W. (2009). Mechanistic niche modelling: combining physiologi-
847 cal and spatial data to predict species’ ranges. *Ecology letters*, 12(4):334–350.
- 848 Kettle, H. and Nutter, D. (2015). stagePop: modelling stage-structured popula-
849 tions in R. *Methods in Ecology and Evolution*, 6(12):1484–1490. _eprint:
850 <https://besjournals.onlinelibrary.wiley.com/doi/pdf/10.1111/2041-210X.12445>.
- 851 Kilpatrick, A. M., Kramer, L. D., Campbell, S. R., Alleyne, E. O., Dobson, A. P., and
852 Daszak, P. (2005). West Nile Virus risk assessment and the bridge vector paradigm.
853 11(3):425–429.

- 854 Koch, L. K., Cunze, S., Werblow, A., Kochmann, J., Dörge, D. D., Mehlhorn, H., and
855 Klimpel, S. (2016). Modeling the habitat suitability for the arbovirus vector *Aedes*
856 *albopictus* (Diptera: Culicidae) in Germany. *Parasitology research*, 115(3):957–964.
- 857 Koenraadt, C. J. M. and Harrington, L. C. (2008). Flushing effect of rain on container-
858 inhabiting mosquitoes *Aedes aegypti* and *Culex pipiens* (Diptera: Culicidae). 45(1):28–
859 35.
- 860 Kraemer, M. U., Reiner, R. C., Brady, O. J., Messina, J. P., Gilbert, M., Pigott, D. M., Yi,
861 D., Johnson, K., Earl, L., Marczak, L. B., et al. (2019). Past and future spread of the
862 arbovirus vect*Aedes aegypti* and *Aedes albopictus*. *Nature microbiology*, 4(5):854–863.
- 863 Kraemer, M. U., Sinka, M. E., Duda, K. A., Mylne, A., Shearer, F. M., Brady, O. J.,
864 Messina, J. P., Barker, C. M., Moore, C. G., Carvalho, R. G., et al. (2015). The global
865 compendium of *Aedes aegypti* and *Ae. albopictus* occurrence. *Scientific data*, 2(1):1–8.
- 866 Kramer, I. M., Kreß, A., Klingelhöfer, D., Scherer, C., Phuyal, P., Kuch, U., Ahrens, B.,
867 Groneberg, D. A., Dhimal, M., and Müller, R. (2020). Does winter cold really limit the
868 dengue vector *Aedes aegypti* in Europe? *Parasites & vectors*, 13(1):1–13.
- 869 Kramer, I. M., Pfeiffer, M., Steffens, O., Schneider, F., Gerger, V., Phuyal, P., Braun,
870 M., Magdeburg, A., Ahrens, B., Groneberg, D. A., et al. (2021). The ecophysiological
871 plasticity of *Aedes aegypti* and *Aedes albopictus* concerning overwintering in cooler
872 ecoregions is driven by local climate and acclimation capacity. *Science of The Total*
873 *Environment*, 778:146128.
- 874 Krupa, E., Henon, N., and Mathieu, B. (2021). Diapause characterisation and seasonality
875 of *Aedes japonicus japonicus* (Diptera, Culicidae) in the Northeast of France. *Parasite*,
876 28.
- 877 Kurucz, K., Manica, M., Delucchi, L., Kemenesi, G., and Marini, G. (2020). Dynamics
878 and distribution of the invasive mosquito *Aedes koreicus* in a temperate European city.
879 *International journal of environmental research and public health*, 17(8):2728.
- 880 Lacour, G., Chanaud, L., L’Ambert, G., and Hance, T. (2015). Seasonal synchronization of
881 diapause phases in *Aedes albopictus* (Diptera: Culicidae). *PloS one*, 10(12):e0145311.
- 882 Lega, J., Brown, H. E., and Barrera, R. (2017). *Aedes aegypti* (Diptera: Culicidae) abun-
883 dance model improved with relative humidity and precipitation-driven egg hatching.
884 *Journal of medical entomology*, 54(5):1375–1384.

- 885 Leta, S., Beyene, T. J., De Clercq, E. M., Amenu, K., Kraemer, M. U., and Revie, C. W.
886 (2018). Global risk mapping for major diseases transmitted by *Aedes aegypti* and *Aedes*
887 *albopictus*. *International Journal of Infectious Diseases*, 67:25–35.
- 888 Liu-Helmersson, J., Rocklöv, J., Sewe, M., and Brännström, Å. (2019). Climate change
889 may enable *Aedes aegypti* infestation in major european cities by 2100. *Environmental*
890 *research*, 172:693–699.
- 891 Lounibos, L. P. and Kramer, L. D. (2016). Invasiveness of *Aedes aegypti* and *Aedes al-*
892 *bopictus* and vectorial capacity for chikungunya virus. *The Journal of infectious dis-*
893 *eases*, 214(suppl_5):S453–S458.
- 894 Maclean, I. M., Mosedale, J. R., and Bennie, J. J. (2019). Microclima: An R package for
895 modelling meso-and microclimate. *Methods in Ecology and Evolution*, 10(2):280–290.
- 896 Magori, K., Legros, M., Puente, M. E., Focks, D. A., Scott, T. W., Lloyd, A. L., and Gould,
897 F. (2009). Skeeter Buster: A Stochastic, Spatially Explicit Modeling Tool for Studying
898 *Aedes aegypti* Population Replacement and Population Suppression Strategies. *PLOS*
899 *Neglected Tropical Diseases*, 3(9):e508.
- 900 Marcantonio, M., Metz, M., Baldacchino, F., Arnoldi, D., Montarsi, F., Capelli, G., Carlin,
901 S., Neteler, M., and Rizzoli, A. (2016). First assessment of potential distribution and
902 dispersal capacity of the emerging invasive mosquito *Aedes koreicus* in Northeast Italy.
903 *Parasites & Vectors*, 9(1):63.
- 904 Marcantonio, M., Reyes, T., and Barker, C. M. (2019). Quantifying *Aedes aegypti* disper-
905 sal in space and time: a modeling approach. *Ecosphere*, 10(12):e02977.
- 906 Marini, F., Caputo, B., Pombi, M., Travaglio, M., Montarsi, F., Drago, A., Rosà, R.,
907 Manica, M., and Torre, A. d. (2019a). Estimating Spatio-Temporal Dynamics of *Aedes*
908 *albopictus* Dispersal to Guide Control Interventions in Case of Exotic Arboviruses in
909 Temperate Regions. *Scientific Reports*, 9(1):1–9.
- 910 Marini, G., Arnoldi, D., Baldacchino, F., Capelli, G., Guzzetta, G., Merler, S., Montarsi,
911 F., Rizzoli, A., and Rosà, R. (2019b). First report of the influence of temperature on the
912 bionomics and population dynamics of *Aedes koreicus*, a new invasive alien species in
913 Europe. *Parasites & vectors*, 12(1):1–12.
- 914 Marini, G., Manica, M., Arnoldi, D., Inama, E., Rosà, R., and Rizzoli, A. (2020). Influence
915 of temperature on the life-cycle dynamics of *Aedes albopictus* population established at
916 temperate latitudes: A laboratory experiment. *Insects*, 11(11):808.

- 917 Martinet, J.-P., Ferté, H., Failloux, A.-B., Schaffner, F., and Depaquit, J. (2019).
918 Mosquitoes of north-western Europe as potential vectors of arboviruses: a review.
919 *Viruses*, 11(11):1059.
- 920 Mathewson, P. D., Moyer-Horner, L., Beever, E. A., Briscoe, N. J., Kearney, M., Yahn,
921 J. M., and Porter, W. P. (2017). Mechanistic variables can enhance predictive models
922 of endotherm distributions: the American pika under current, past, and future climates.
923 *Global Change Biology*, 23(3):1048–1064.
- 924 McBride, C. S., Baier, F., Omondi, A. B., Spitzer, S. A., Lutomiah, J., Sang, R., Ignell, R.,
925 and Vosshall, L. B. (2014a). Evolution of mosquito preference for humans linked to an
926 odorant receptor. *Nature*, 515(7526):222–227.
- 927 McBride, C. S., Baier, F., Omondi, A. B., Spitzer, S. A., Lutomiah, J., Sang, R., Ignell, R.,
928 and Vosshall, L. B. (2014b). Evolution of mosquito preference for humans linked to an
929 odorant receptor. *Nature*, 515(7526):222–227.
- 930 McKenzie, B. A., Wilson, A. E., and Zohdy, S. (2019). *Aedes albopictus* is a competent
931 vector of Zika virus: A meta-analysis. *PLOS ONE*, 14(5):e0216794. Publisher: Public
932 Library of Science.
- 933 Metelmann, S., Caminade, C., Jones, A. E., Medlock, J. M., Baylis, M., and Morse, A. P.
934 (2019). The UK’s suitability for *Aedes albopictus* in current and future climates. *Journal*
935 *of The Royal Society Interface*, 16(152):20180761. Publisher: Royal Society.
- 936 Montarsi, F., Ciocchetta, S., Devine, G., Ravagnan, S., Mutinelli, F., Frangipane Di Re-
937 galbono, A., Otranto, D., and Capelli, G. (2015a). Development of *Dirofilaria immitis*
938 within the mosquito *Aedes (Finlaya) koreicus*, a new invasive species for Europe. *Par-*
939 *asites and Vectors*, 8(1).
- 940 Montarsi, F., Drago, A., Dal Pont, M., Delai, N., Carlin, S., Cazzin, S., Ciocchetta, S.,
941 Arnoldi, D., Baldacchino, F., Rizzoli, A., et al. (2014). Current knowledge on the
942 distribution and biology of the recently introduced invasive mosquito *Aedes koreicus*
943 (Diptera: Culicidae). *Firenze (Italy): Atti Accademia Nazionale Italiana di Entomolo-*
944 *gia*, 62:169–174.
- 945 Montarsi, F., Drago, A., Martini, S., Calzolari, M., De Filippo, F., Bianchi, A., Mazzucato,
946 M., Ciocchetta, S., Arnoldi, D., Baldacchino, F., et al. (2015b). Current distribution of
947 the invasive mosquito species, *Aedes koreicus* [*Hulecoeteomyia koreica*] in Northern
948 Italy. *Parasites & vectors*, 8(1):1–5.

- 949 Montarsi, F., Martini, S., Dal Pont, M., Delai, N., Milone, N. F., Mazzucato, M., Sop-
950 pelsa, F., Cazzola, L., Cazzin, S., Ravagnan, S., et al. (2013). Distribution and habitat
951 characterization of the recently introduced invasive mosquito *Aedes koreicus* [*Hulecoe-*
952 *teomyia koreica*], a new potential vector and pest in north-eastern italy. *Parasites &*
953 *vectors*, 6(1):1–10.
- 954 Müller, P., Engeler, L., Vavassori, L., Suter, T., Guidi, V., Gschwind, M., Tonolla, M.,
955 and Flacio, E. (2020). Surveillance of invasive *Aedes* mosquitoes along Swiss traffic
956 axes reveals different dispersal modes for *Aedes albopictus* and *Ae. japonicus*. *PLoS*
957 *neglected tropical diseases*, 14(9):e0008705.
- 958 Müller, R., Knautz, T., Vollroth, S., Berger, R., Kreß, A., Reuss, F., Groneberg, D. A.,
959 and Kuch, U. (2018). Larval superiority of *Culex pipiens* to *Aedes albopictus* in a
960 replacement series experiment: prospects for coexistence in Germany. *Parasites &*
961 *vectors*, 11(1):1–16.
- 962 Muñoz-Sabater, J., Dutra, E., Agustí-Panareda, A., Albergel, C., Arduini, G., Balsamo,
963 G., Boussetta, S., Choulga, M., Harrigan, S., Hersbach, H., et al. (2021). ERA5-Land:
964 A state-of-the-art global reanalysis dataset for land applications. *Earth System Science*
965 *Data Discussions*, pages 1–50.
- 966 Näslund, J., Ahlm, C., Islam, K., Evander, M., Bucht, G., and Lwande, O. W. (2021).
967 Emerging mosquito-borne viruses linked to *Aedes aegypti* and *Aedes albopictus*: Global
968 status and preventive strategies. *Vector-Borne and Zoonotic Diseases*, 21(10):731–746.
- 969 Negri, A., Arnoldi, I., Brilli, M., Bandi, C., Gabrieli, P., and Epis, S. (2021). Evidence for
970 the spread of the alien species *Aedes koreicus* in the Lombardy region, Italy. *Parasites*
971 *& Vectors*, 14(1):1–6.
- 972 Oliveira, S., Rocha, J., Sousa, C. A., and Capinha, C. (2021). Wide and increasing suit-
973 ability for *Aedes albopictus* in Europe is congruent across distribution models. *Scientific*
974 *reports*, 11(1):1–9.
- 975 Onofri, A. (2020). *aomisc: Statistical methods for the agricultural sciences*. R package
976 version 0.64.
- 977 Otero, M., Solari, H. G., and Schweigmann, N. (2006). A stochastic population dynamics
978 model for *Aedes aegypti*: formulation and application to a city with temperate climate.
979 *Bulletin of mathematical biology*, 68(8):1945–1974.

- 980 Pasaoglu, G., Fiorello, D., Martino, A., Scarcella, G., Alemanno, A., Zubaryeva, A., and
981 Thiel, C. (2012). Driving and parking patterns of European car drivers-a mobility sur-
982 vey. *Luxembourg: European Commission Joint Research Centre*.
- 983 Pasquali, S., Mariani, L., Calvitti, M., Moretti, R., Ponti, L., Chiari, M., Sperandio, G.,
984 and Gilioli, G. (2020). Development and calibration of a model for the potential estab-
985 lishment and impact of *Aedes albopictus* in Europe. *Acta tropica*, 202:105228.
- 986 Peterson, A. T. (2014). *Mapping disease transmission risk: enriching models using bio-*
987 *geography and ecology*. JHU Press.
- 988 Petrić, M., Ducheyne, E., Gossner, C. M., Marsboom, C., Nicolas, G., Venail, R., Hen-
989 drickx, G., and Schaffner, F. (2021). Seasonality and timing of peak abundance of *Aedes*
990 *albopictus* in Europe: Implications to public and animal health. *Geospatial Health*,
991 16(1).
- 992 Powell, J. R., Tabachnick, W. J., Powell, J. R., and Tabachnick, W. J. (2013). History of
993 domestication and spread of *Aedes aegypti* - A Review. *Memórias do Instituto Oswaldo*
994 *Cruz*, 108:11–17.
- 995 Pumpuni, C. B., Knepler, J., and Craig, G. B. (1992). Influence of temperature and larval
996 nutrition on the diapause inducing photoperiod of *Aedes albopictus*. *Journal of the*
997 *American Mosquito Control Association*, 8(3):223–227.
- 998 R Core Team (2021). *R: A Language and Environment for Statistical Computing*. R
999 Foundation for Statistical Computing, Vienna, Austria.
- 1000 Reiskind, M. and Lounibos, L. (2013). Spatial and temporal patterns of abundance of
1001 *Aedes aegypti* l.(*Stegomyia aegypti*) and *Aedes albopictus* (skuse)[*Stegomyia albopictus*
1002 (*Skuse*)] in southern florida. *Medical and veterinary entomology*, 27(4):421–429.
- 1003 Reuss, F., Wieser, A., Niamir, A., Bálint, M., Kuch, U., Pfenninger, M., and Müller, R.
1004 (2018). Thermal experiments with the asian bush mosquito (*Aedes japonicus japoni-*
1005 *cus*)(Diptera: Culicidae) and implications for its distribution in Germany. *Parasites &*
1006 *vectors*, 11(1):1–10.
- 1007 Rezza, G., Nicoletti, L., Angelini, R., Romi, R., Finarelli, A. C., Panning, M., Cordioli,
1008 P., Fortuna, C., Boros, S., Magurano, F., Silvi, G., Angelini, P., Dottori, M., Ciufolini,
1009 M. G., Majori, G. C., Cassone, A., and CHIKV study group (2007). Infection with
1010 Chikungunya virus in Italy: an outbreak in a temperate region. *Lancet*, 370(9602):1840–
1011 1846.

- 1012 Ritz, C., Baty, F., Streibig, J. C., and Gerhard, D. (2015). Dose-response analysis using r.
1013 *PLOS ONE*, 10(e0146021).
- 1014 Roche, B., Léger, L., L'Ambert, G., Lacour, G., Foussadier, R., Besnard, G., Barré-Cardi,
1015 H., Simard, F., and Fontenille, D. (2015). The spread of *Aedes albopictus* in metropoli-
1016 tan France: contribution of environmental drivers and human activities and predictions
1017 for a near future. *PloS one*, 10(5):e0125600.
- 1018 Rohatgi, A. (2020). *Webplotdigitizer: Version 4.4*.
- 1019 Roiz, D., Boussès, P., Simard, F., Paupy, C., and Fontenille, D. (2015). Autochthonous
1020 chikungunya transmission and extreme climate events in southern France. *PLoS Ne-*
1021 *glected Tropical Diseases*, 9(6):e0003854.
- 1022 Schaffner, F., Karch, S., et al. (2000). First record of *Aedes albopictus* (Skuse, 1894) in
1023 metropolitan France. *COMPTES RENDUS-ACADEMIE DES SCIENCES PARIS SERIE*
1024 *3*, 323(4):373–376.
- 1025 Schaffner, F., Vazeille, M., Kaufmann, C., Failloux, A.-B., and Mathis, A. (2011). Vec-
1026 tor competence of *Aedes japonicus* for chikungunya and dengue viruses. *European*
1027 *Mosquito Bulletin*, (29):141–142.
- 1028 Schulzweida, U. (2019). Cdo user guide.
- 1029 Scott, J. (2003). *The Ecology of the Exotic Mosquito Ochlerotatus (Finlaya) japonicus*
1030 *japonicus (Theobald 1901) (Diptera: Culicidae) and an Examination of its Role in the*
1031 *West Nile Virus Cycle in New Jersey*. Ph.D. thesis, Rutgers University, New Brunswick,
1032 NJ.
- 1033 Seidel, B., Montarsi, F., Huemer, H. P., Indra, A., Capelli, G., Allerberger, F., and
1034 Nowotny, N. (2016). First record of the Asian bush mosquito, *Aedes japonicus japon-*
1035 *icus*, in Italy: invasion from an established Austrian population. *Parasites & vectors*,
1036 9(1):1–4.
- 1037 Sherpa, S., Blum, M. G., Capblancq, T., Cumer, T., Rioux, D., and Després, L. (2019).
1038 Unravelling the invasion history of the Asian tiger mosquito in Europe. *Molecular*
1039 *Ecology*, 28(9):2360–2377.
- 1040 Souza-Neto, J. A., Powell, J. R., and Bonizzoni, M. (2019). *Aedes aegypti* vector compe-
1041 tence studies: A review. *Infection, Genetics and Evolution*, 67:191–209.
- 1042 Stallman, R. (1985). The GNU Manifesto. *j-DDJ*, 10(3):30–35.

- 1043 Takashima, I. and Rosen, L. (1989). Horizontal and vertical transmission of Japanese
1044 encephalitis virus by *Aedes japonicus* (Diptera: Culicidae). *Journal of Medical Ento-*
1045 *mology*, 26(5):454–458.
- 1046 Takken, W. and van den Berg, H. (2019). Manual on prevention of establishment and
1047 control of mosquitoes of public health importance in the WHO European region (with
1048 special reference to invasive mosquitoes).
- 1049 Tanaka, K., Mizusawa, K., and Saugstad, E. S. (1979a). A revision of the adult and larval
1050 mosquitoes of Japan (including the Ryukyu archipelago and the Ogasawara islands) and
1051 Korea (Diptera: Culicidae). Technical report, ARMY MEDICAL LAB PACIFIC APO
1052 SAN FRANCISCO 96343.
- 1053 Tanaka, T., Mizusawa, K., and Saugstad, E. (1979b). *Mosquitoes of Japan and Korea*,
1054 volume 16 of *Contributions of the American Entomological Institute*. the American
1055 Entomological Institute.
- 1056 Thomas, S. M., Obermayr, U., Fischer, D., Kreyling, J., and Beierkuhnlein, C. (2012).
1057 Low-temperature threshold for egg survival of a post-diapause and non-diapause Eu-
1058 ropean aedine strain, *Aedes albopictus* (Diptera: Culicidae). *Parasites & Vectors*,
1059 5(1):100.
- 1060 Thornton, M., Shrestha, R., Wei, Y., Thornton, P., Kao, S., and Wilson, B. (2020). Daymet-
1061 Daymet: Daily Surface Weather Data on a 1-km Grid for North America, Version 4.
1062 Artwork Size: 0 MB Medium: netCDF Publisher: ORNL Distributed Active Archive
1063 Center Version Number: 4.
- 1064 Tran, A., l’Ambert, G., Lacour, G., Benoît, R., Demarchi, M., Cros, M., Cailly, P., Aubry-
1065 Kientz, M., Balenghien, T., and Ezanno, P. (2013). A rainfall-and temperature-driven
1066 abundance model for *Aedes albopictus* populations. *International journal of environ-*
1067 *mental research and public health*, 10(5):1698–1719.
- 1068 Tran, A., Mangeas, M., Demarchi, M., Roux, E., Degenne, P., Haramboure, M., Le Goff,
1069 G., Damiens, D., Gouagna, L.-C., Herbreteau, V., et al. (2020). Complementarity of
1070 empirical and process-based approaches to modelling mosquito population dynamics
1071 with *Aedes albopictus* as an example—application to the development of an operational
1072 mapping tool of vector populations. *PloS one*, 15(1):e0227407.
- 1073 Tripet, F., Lounibos, L. P., Robbins, D., Moran, J., Nishimura, N., and Blosser, E. M.
1074 (2011). Competitive reduction by satyrization? evidence for interspecific mating in

- 1075 nature and asymmetric reproductive competition between invasive mosquito vectors.
1076 *The American journal of tropical medicine and hygiene*, 85(2):265–270.
- 1077 Tsigkinopoulou, A., Hawari, A., Uttley, M., and Breitling, R. (2018). Defining informative
1078 priors for ensemble modeling in systems biology. *Nature Protocols*, 13(11):2643.
- 1079 Turell, M. J., Beaman, J. R., and Neely, G. W. (1994). Experimental transmission of
1080 eastern equine encephalitis virus by strains of *Aedes albopictus* and *A. taeniorhynchus*
1081 (Diptera: Culicidae). *Journal of Medical Entomology*, 31(2):287–290.
- 1082 Urbanski, J., Mogi, M., O'Donnell, D., DeCotiis, M., Toma, T., and Armbruster, P. (2012).
1083 Rapid adaptive evolution of photoperiodic response during invasion and range expansion
1084 across a climatic gradient. *The American Naturalist*, 179(4):490–500.
- 1085 Venturi, G., Luca, M. D., Fortuna, C., Remoli, M. E., Riccardo, F., Severini, F., Toma,
1086 L., Manso, M. D., Benedetti, E., Caporali, M. G., Amendola, A., Fiorentini, C., Lib-
1087 erato, C. D., Giammattei, R., Romi, R., Pezzotti, P., Rezza, G., and Rizzo, C. (2017).
1088 Detection of a chikungunya outbreak in Central Italy, August to September 2017. *Euro-*
1089 *surveillance*, 22(39):17–00646.
- 1090 Veronesi, E., Paslaru, A., Silaghi, C., Tobler, K., Glavinic, U., Torgerson, P., and Mathis,
1091 A. (2018). Experimental evaluation of infection, dissemination, and transmission rates
1092 for two West Nile virus strains in European *Aedes japonicus* under a fluctuating temper-
1093 ature regime. *Parasitology research*, 117(6):1925–1932.
- 1094 Versteirt, V., De Clercq, E. M., Fonseca, D. M., Pecor, J., Schaffner, F., Coosemans, M.,
1095 and Van Bortel, W. (2012). Bionomics of the Established Exotic Mosquito Species
1096 *Aedes koreicus* in Belgium, Europe. *Journal of Medical Entomology*, 49(6):1226–1232.
- 1097 Versteirt, V., Schaffner, F., Garros, C., Dekoninck, W., Coosemans, M., and Van Bor-
1098 tel, W. (2009). Introduction and establishment of the exotic mosquito species *Aedes*
1099 *japonicus japonicus* (Diptera: Culicidae) in Belgium. *Journal of Medical Entomology*,
1100 46(6):1464–1467.
- 1101 Waldock, J., Chandra, N. L., Lelieveld, J., Proestos, Y., Michael, E., Christophides, G.,
1102 and Parham, P. E. (2013). The role of environmental variables on *Aedes albopictus*
1103 biology and chikungunya epidemiology. *Pathogens and global health*, 107(5):224–241.
- 1104 Watson, M. S. (1967). *Aedes (Stegomyia) albopictus* (Skuse): A Literature Review. *Mis-*
1105 *cellaneous publication*, 22:42.

- 1106 Werner, D., Zielke, D., and Kampen, H. (2016). First record of *Aedes koreicus* (Diptera:
1107 Culicidae) in Germany. *Parasitology Research*, 115(3):1331–1334.
- 1108 Westby, K. M., Fritzen, C., Paulsen, D., Poindexter, S., and Moncayo, A. C. (2015). La
1109 Crosse encephalitis virus infection in field-collected *Aedes albopictus*, *Aedes japoni-*
1110 *cus*, and *Aedes triseriatus* in Tennessee. *Journal of the American Mosquito Control*
1111 *Association*, 31(3):233–241.
- 1112 Wieser, A., Reuss, F., Niamir, A., Müller, R., O’Hara, R. B., and Pfenninger, M. (2019).
1113 Modelling seasonal dynamics, population stability, and pest control in *Aedes japonicus*
1114 *japonicus* (Diptera: Culicidae). *Parasites & vectors*, 12(1):1–12.

1115 **A Review of mechanistic model for invasive *Aedes***

Name	Year	Species	Biological resolution	Time	Space	Programming language	Reference
SkeeterBooster	2009	<i>Ae. aegypti</i>	Agent-based			C++	Magori et al. (2009)
stagePop	2009		Process-based			R	Kettle and Nutter (2015)
sPop	2018					C++, R, Python	Erguler (2018)
albopictus	2019	<i>Ae. albopictus</i>	Process-based			C++, R, Python 4	Erguler et al. (2016, 2017)
	2019	<i>Ae. albopictus</i>	Process-based			Octave v4.2.1, Runge-Kutta 4	Metelmann et al. (2019)
	2019	<i>Ae. albopictus</i>	Process-based			R, Ocelet	Tran et al. (2013, 2020)
	2020	<i>Ae. aegypti</i>	Process-based			R	Iwamura et al. (2020)
	2020	<i>Ae. koreicus</i>	Process-based			R	Kurucz et al. (2020)

Table 2: Description of mechanistic codes for invasive *Aedes* made available as software or scripts.

1116 **B Parameters used in dynamAedes**

Species	Stage	Parameters	Main source	data	Origin	Value	Comments
<i>Ae. aegypti</i> and <i>Ae. albopictus</i>	Eggs	min number of days for eggs development	Christophers 1960; Delatte et al 2009		Literature therein; Reunion (France)	La 4	
<i>Ae. aegypti</i> and <i>Ae. albopictus</i>	Juveniles	min number of days for imma- ture development	Christophers 1960; Delatte et al 2009		Literature therein; Reunion (France)	La 6	
<i>Ae. aegypti</i> and <i>Ae. albopictus</i>	Adults	min number of days for gonotrophic cycle	Christophers 1960; Delatte et al 2009		Literature therein; Reunion (France)	La 4	
<i>Ae. koreicus</i> and <i>Ae. japonicus</i>	Eggs	min number of days for eggs development	Dr Daniele Arnoldi unpublished results for <i>Ae. koreicus</i>		Trento (NE Italy)	8	
<i>Ae. koreicus</i> and <i>Ae. japonicus</i>	Juveniles	min number of days for imma- ture development	Dr Daniele Arnoldi unpublished results for <i>Ae. koreicus</i> ; Wieser et al. (2019)		Trento (NE Italy)	9	min 10 days for <i>Ae. koreicus</i> , min 8 days for <i>Ae. japonicus</i> . Assumed 9 for both species
<i>Ae. koreicus</i> and <i>Ae. japonicus</i>	Adults	min number of days for gonotrophic cycle	Assumed the same of <i>Ae. aegypti</i>		-	4	Since the probability of complete the gonothropic cycle is roughly 1/3 of <i>Ae. aegypti</i> , we kept the same length of <i>Ae. aegypti</i>
All species	Juveniles	Survival rate (density-dependent)	Hancock et al. 2016		Tropical (NE Australia)		1-density dependant survival rate is additive to 1-temperature-dependent survival rate; the estimates made for <i>Ae. aegypti</i> were extended to the other three species
	Adults	Sex ratio 1:1	-		-		General modelling assumption widely taken in process-based modelling literature

Table 3: Other model features

Species	Stage	Model parameter	Data source	Origin	Function	Comments
<i>Ae. aegypti</i>	Egg	Survival rate	Thomas et al. 2012, Eisen et al. 2014	Laboratory colony(Tropical Asia origin); Literature review	Beta	Data for T>0 taken from Eisen 2014, data for T<0 taken from Thomas et al. 2012
		Hatching rate	Christophers 1960; Farnesi et al 2009; Mohammed and Chadee 2011	Rock-feller strain; Trinidad and Tobago	Beta	48h estimates from Mohammed and Chadee 2011 divided by two to get a daily rate. Additional data: 0 hatching a 7°C from Christophers and 0.025 at 12°C daily hatching from Farnesi et al. (2009)
	Juvenile	Survival rate (temperature-dependent)	Yang et al. 2009	NW of São Paulo State (Brazil)	Beta	Table 8 from Yang et al. 2009 Appendix I
		Emergence rate	Yang et al. 2009; Grech et al (2015)	NW of São Paulo State (Brazil); Cordoba (Argentina)	Beta	Data from Yang et al. (2009) refer to all immature stages, we corrected them to match only pupa using information present in Grech et al (2015) by taking the ratio between the minimum pupation time of the two experiment as a scaling factor
	Adult	Survival rate	Yang et al. 2009	NW of São Paulo State (Brazil)	Beta	Table 4
		Gonotrophic cycle	Yang et al. 2009	NW of São Paulo State (Brazil)	Beta	Table 5
<i>Ae. albopictus</i>	Egg	Oviposition: number of eggs	Christophers 1960; Yang et al. 2009	Literature therein; NW of São Paulo State (Brazil)	Beta	Table 5 from Yang et al (2009) rescaled using the average number of eggs/female reported in Christophers (1960)
		Survival rate (non-diapausing)	Metelmann et al. 2019; Expert based	Literature therein	nonlinear	Polynomial function taken from the SM manually adapted to get no survival at T>40°C
	Survival rate (diapausing)	Metelmann et al. 2019	Literature therein	nonlinear	Polynomial function taken from the SM	
	Hatching rate ((non-diapausing)	Delatte et al. 2009	La Reunion (France)	Beta	Table 1; column Egg-L1	
	Hatching rate (diapausing)	-	-	-	-	Assumed the same as for non-diapausing eggs
	Survival rate (temperature-dependent)	Metelmann et al. 2019	Literature therein	nonlinear	Polynomial function taken from the SM	
Juvenile	Emergence rate	Delatte et al. 2009	La Reunion (France)	Beta	Table 1; column Pupae-adult	
Adult	Survival rate	Metelmann et al. 2019	Literature therein	nonlinear	Polynomial function taken from the SM	
	Gonotrophic cycle	Delatte et al. 2009	La Reunion (France)	Beta	Table 6	

Species	Stage	Model parameter	Data source	Origin	Function	Comments
<i>Ae. japonicus</i>	Egg	Oviposition: number of eggs	Delatte et al. 2009	La Reunion (France)	Beta	Table 6
		Survival rate	Wieser et al. 2019	Biberach (Germany)	Beta	Observation taken from Fig. 1 in Wieser et al (2019)
	Juvenile	Hatch rate	Wieser et al. 2019	Biberach (Germany)	Beta	Reuss et al., unpublished. Hatching observed also below a thin ice layer (T<0)
		Survival rate	Wieser et al. 2019	Biberach (Germany)	Beta	Reuss et al., unpublished
		Emergence rate	Reuss et al. 2018 SM	Biberach (Germany)	Beta	Table S2; survival upper temperature limit was adapted by accounting for expert opinion.
		Survival rate	Reuss et al. 2018 SM	Biberach (Germany)	Beta	Fig. 2
	Adult	Gonotrophic cycle	-	-	Beta	No information available, assumed the same of <i>Ae. koreicus</i> due to their phylogenetic and biogeographic similarity
	Egg	Oviposition: number of eggs	Reuss et al. 2018	Biberach (Germany)	Beta	Number of eggs estimated by mean female wing length, using the formula taken from Armistead et al. (2009), their Fig. 5; we divided the estimated eggs per female per gonotrophic cycle by a factor of two, due the two ovipositing days we are accounting in the model.
		Survival rate	Marini et al. 2019; Expert Based	Trento (NE Italy)	nonlinear	Polynomial function F3 and parameters values taken from Tab. 5 in Marini et al (2019) adjusted using observations provided in Arnoldi et al., unpublished observations
		Hatching rate	Marini et al. 2019; Expert Based	Trento (NE Italy)	Beta	Table 1 scaled with unpublished data to account for non-embryonated eggs; Arnoldi et al., unpublished observations
Survival rate (temperature-dependent)		Marini et al. 2019; Expert Based	Trento (NE Italy)	Beta	Table 1 averaged from instar 1 to 4; the the upper limit has been adapted accordingly to expert opinions by Ciocchetta et al., unpublished observations and Arnoldi et al., unpublished observations	
Emergence rate		Marini et al. 2019; Expert Based	Trento (NE Italy)	Beta	Table 2	
Survival rate		Marini et al. 2019; Expert Based	Trento (NE Italy)	Beta	Table 3	
Adult	Gonotrophic cycle	Marini et al. 2019; Expert Based	Trento (NE Italy)	Beta	Table 3	
	Oviposition: number of eggs	Marini et al. 2019; Expert Based	Trento (NE Italy)	Beta	Arnoldi et al., unpublished observations	

Table 4: Species-specific temperature-dependent physiological parameters

Species	Stage	Parameters	Main source	Origin	Distribution	Comments
<i>Ae. aegypti</i>	Adults	Active dispersal	Marcantonio et al. 2019	California (USA)	Log-normal	Table 3
<i>Ae. albopictus</i>	Adults	Active dispersal	Marini et al. 2019B	Rome (Italy)	Log-normal	Figure 2a; Data from the 3 MRR were fit with several distributions, best distribution chosen using AIC
<i>Ae. japonicus</i>	Adults	Active dispersal	-	-	Log-normal	No information available, assumed the same of <i>Ae. albopictus</i>
<i>Ae. koreicus</i>	Adults	Active dispersal	-	-	Log-normal	No information available, assumed the same of <i>Ae. albopictus</i>
All species	All species	Passive dispersal (average trip distance)	Pasaoglu et al. 2012	-	-	Trip distance weighted average for ITA, DEU, FRA, ESP, POL, UK. Data taken from Figure 4.4 Average trip distance (km) by trip purpose using WebPlotDigitalizer
All species	Adults	Passive dispersal (Hitchhiking probability)	Ertijia et al. 2017	Mediterranean (Catalonia, Spain)	gamma distribution	0.0051 probability of a female mosquito to enter a car; Assumed to be the same for all the species as estimated by Ertijia et al. 2017 for <i>Ae. albopictus</i>

Table 5: Species specific dispersal parameters

Species	Stage	Model parameter	Data source	Origin	Function	Comments
<i>Ae. aegypti</i>	Diapause Egg	Diapause incidence	Lacour et al. 2015	Ovitrap (Provence, Southern France)	Exponential	
<i>Ae. japonicus</i>	Diapause Egg	Diapause incidence	Krupa et al. 2021	Ovitrap (Bas-Rhin, Northeast France)	Exponential	
<i>Ae. kor-eicus</i>	Diapause Egg	Diapause incidence	Krupa et al. 2021	Ovitrap (Bas-Rhin, Northeast France)	Exponential	We used the same exponential function used for <i>Ae. japonicus</i> due to the close phylogenetic relationship between these two species

Table 6: Species specific photoperiod parameters

1117 **A** *Aedes sp.* response curve

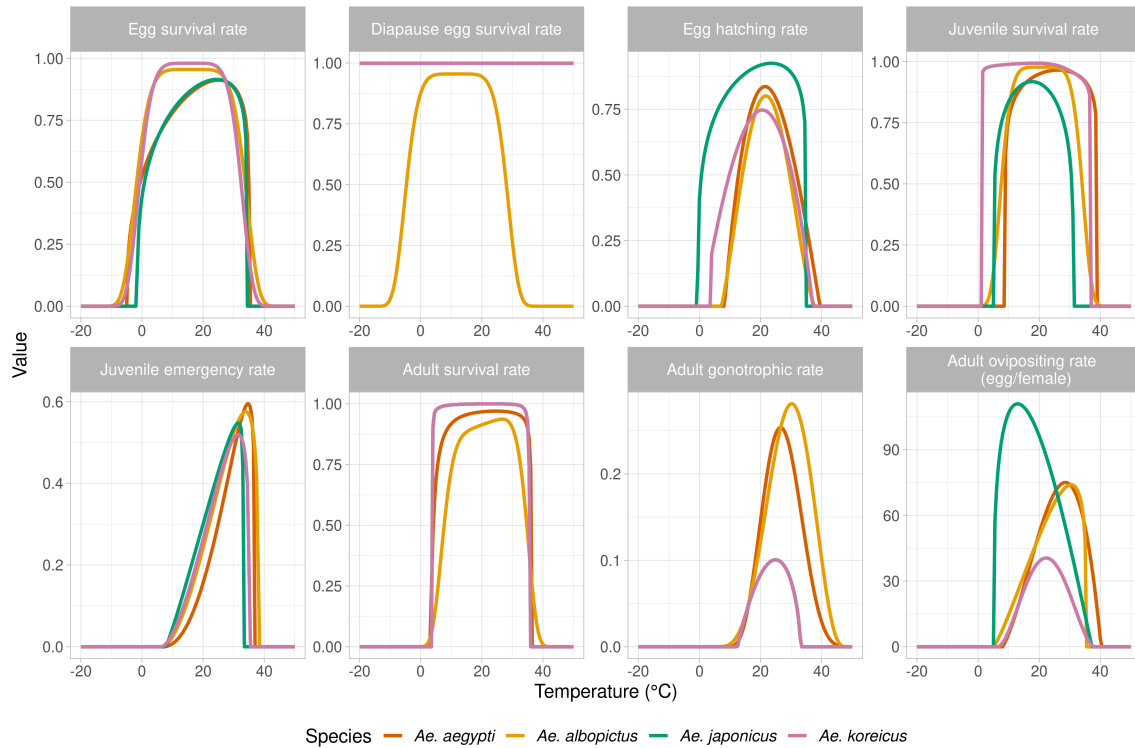


Figure 7: Overview of the temperature-dependent functions used in the model for the four *Aedes* species

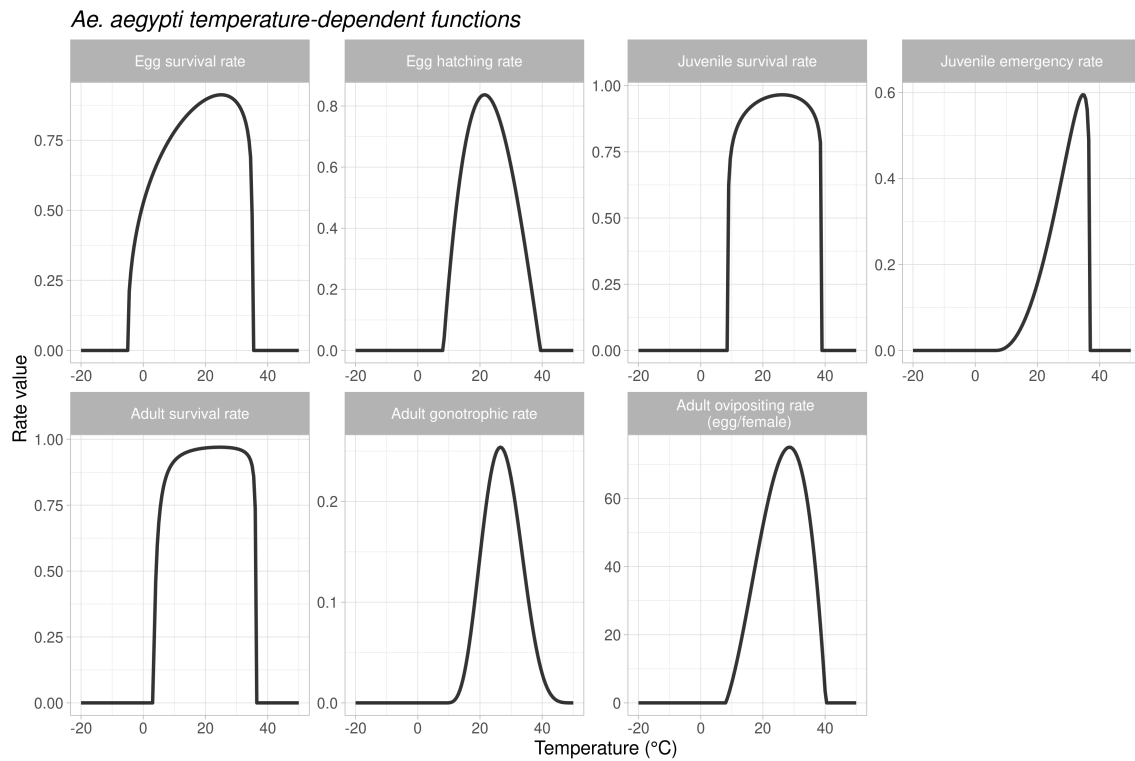


Figure 8: Overview of the temperature-dependent functions used in the model for *Ae. aegypti*

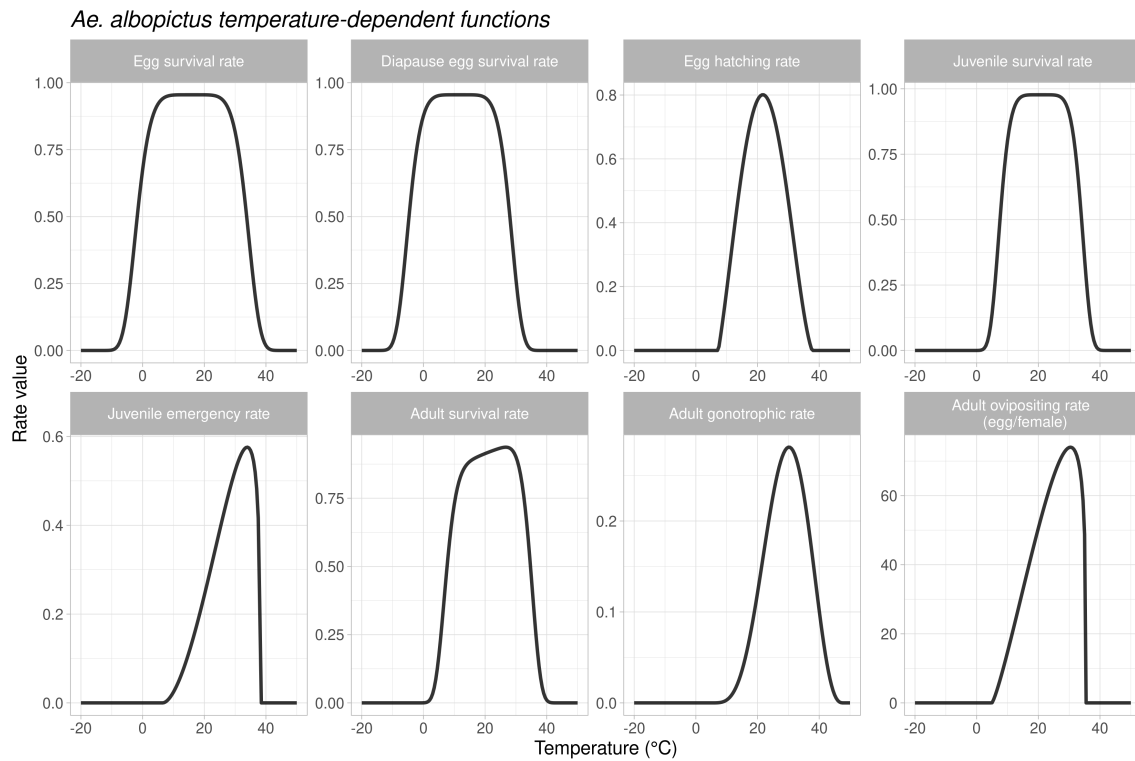


Figure 9: Overview of the temperature-dependent functions used in the model for *Ae. albopictus*

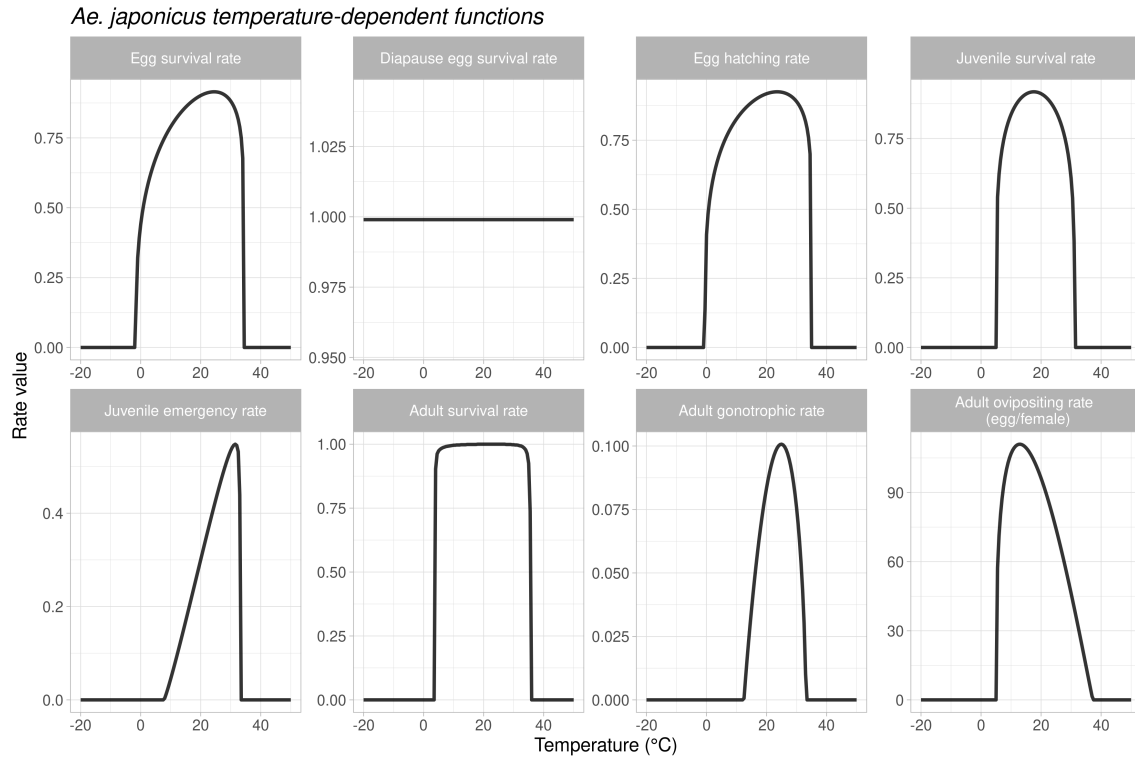


Figure 10: Overview of the temperature-dependent functions used in the model for *Ae. japonicus*

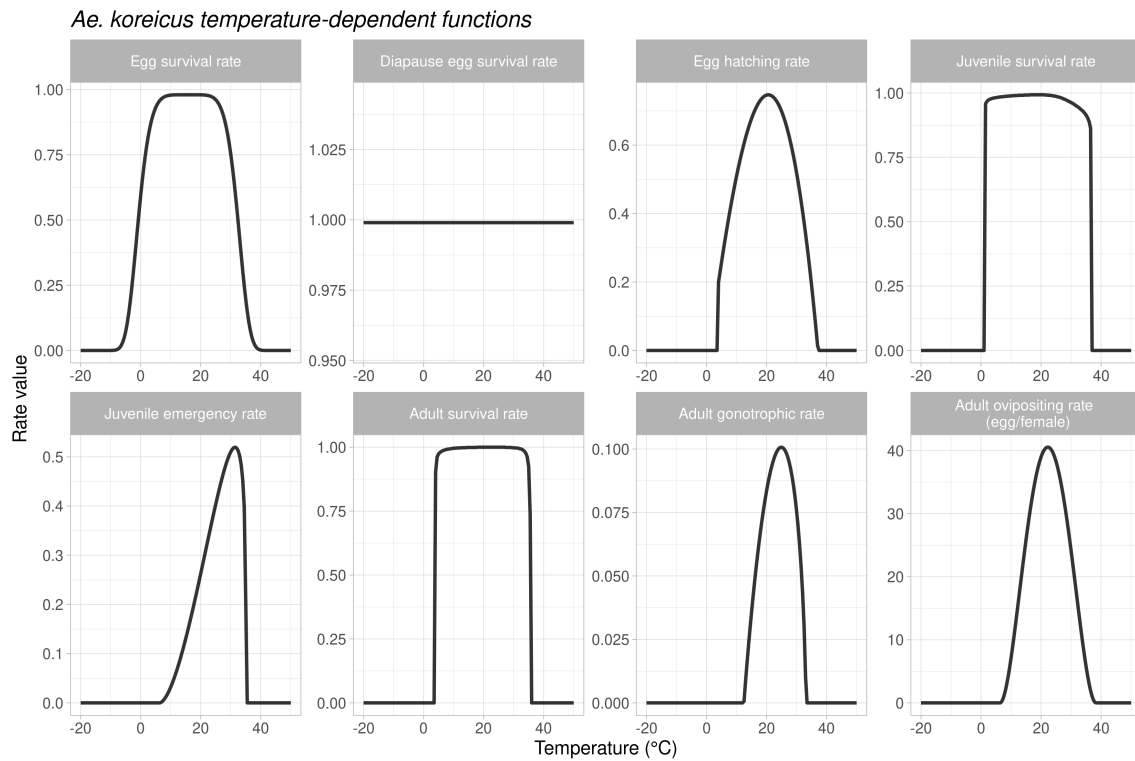


Figure 11: Overview of the temperature-dependent functions used in the model for *Ae. koreicus*

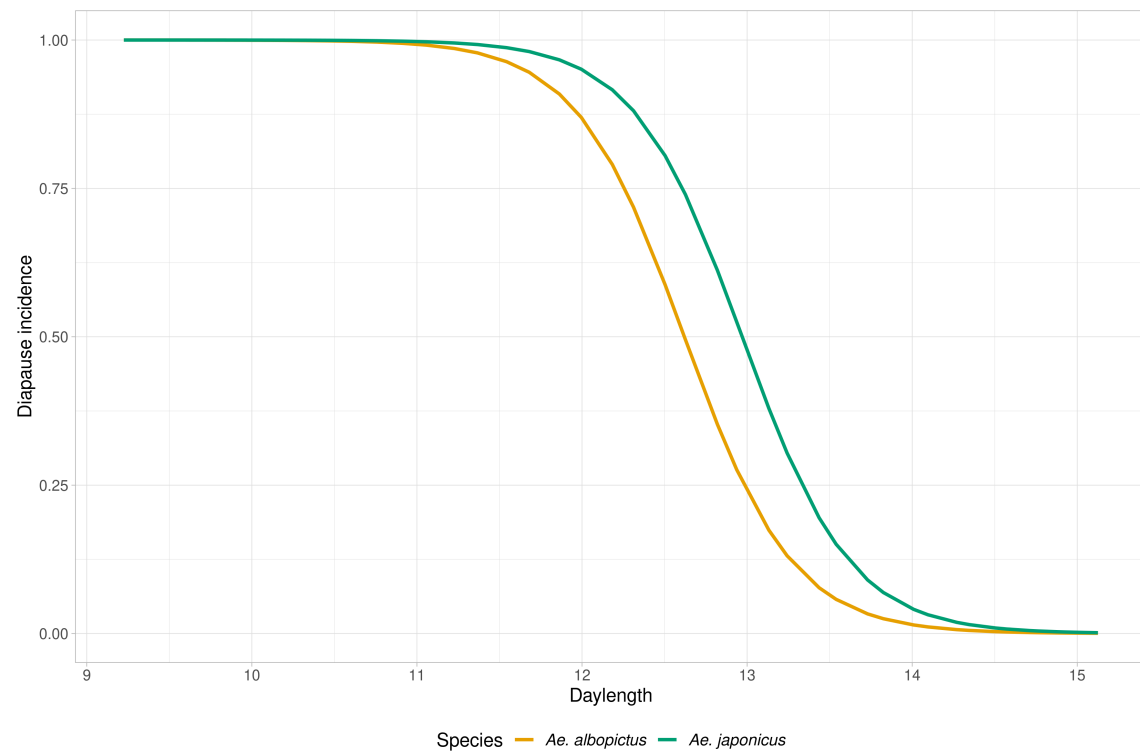


Figure 12: Overview of the photoperiod-dependent diapause incidence function used to in the model for *Ae. albopictus* and *Ae. japonicus*. The *Ae. japonicus* function was used for *Ae. koreicus* as well.

1118 **B Larval habitat water volume parameter sensitivity**

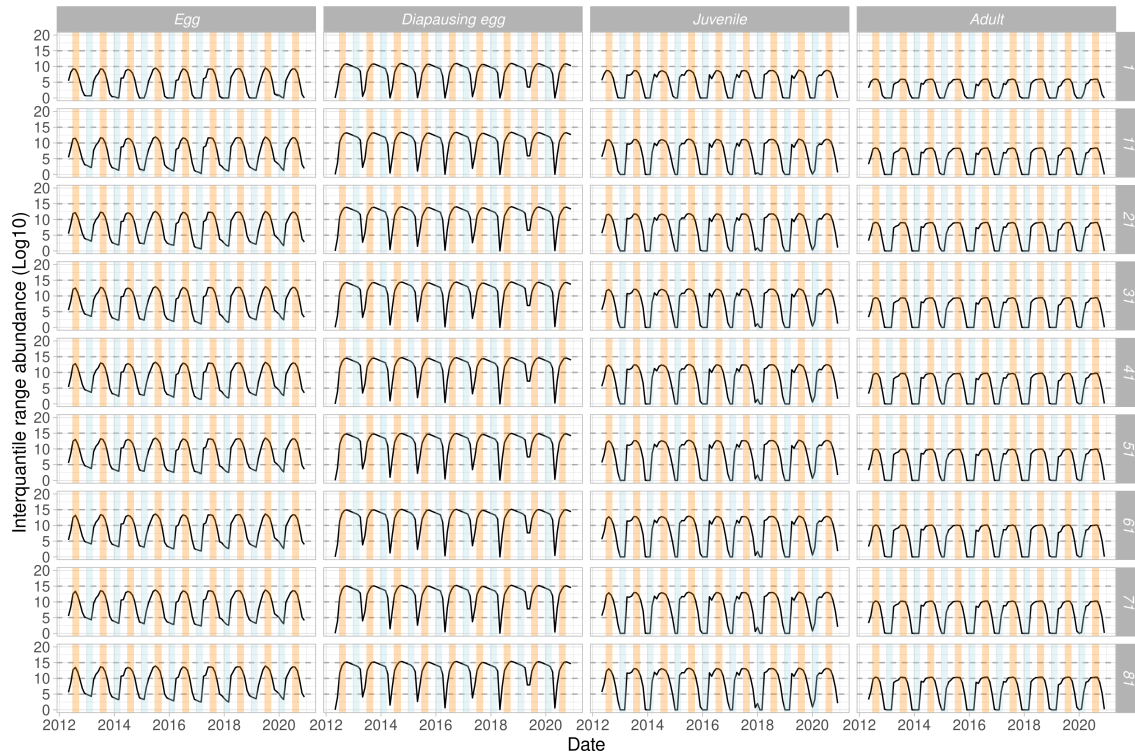


Figure 13: Sensitivity analysis on the effect of the $1hvw$ parameter on the estimated number of individuals. In this example, we used the temperature observations of the Nice weather station used in the case study and varied the amount of water volume. The seasonal trend remained the same but, as expected, the simulated number of individuals increase as the $1hvw$ parameter increase.

1119 **C** *Aedes aegypti* and *Ae. albopictus* regional scale case
1120 study

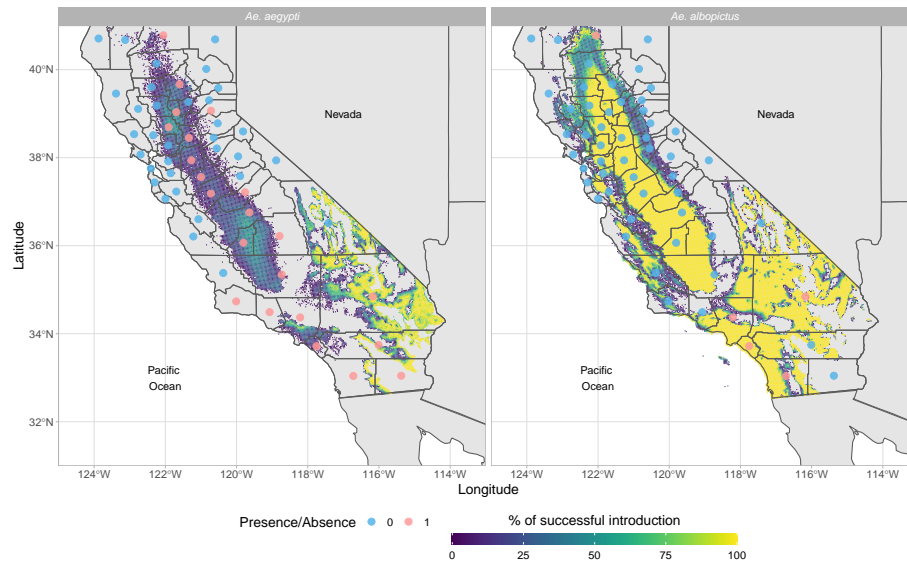


Figure 14: Predicted percentage of establishment of *Ae. aegypti* *Ae. albopictus* in California (USA) for the years 2011-2016 and 2013-2018, respectively. Only pixels having a probability of successful introduction >0 are shown. The red dots represent the counties where the species have been found.

1121 **D** *Aedes koreicus* population dynamics punctual scale case
 1122 study

Year	Month	CI 2.5%	CI 25%	CI 50%	CI 75%	CI 97.5%	Observed <i>Ae. Koreicus</i>
2016	May	0.00	1.45	5.26	13.74	31.22	2
2016	June	0.00	1.37	6.36	14.40	40.64	5
2016	July	0.00	2.32	11.85	32.62	101.76	3
2016	August	0.70	24.57	66.65	128.03	266.00	9
2016	September	0.18	14.52	37.37	88.27	175.66	37
2016	October	0.00	0.24	1.18	3.14	10.17	0
2017	May	0.02	0.51	2.67	7.85	18.44	9
2017	June	0.29	2.75	10.60	28.57	55.28	8
2017	July	3.67	10.91	30.62	85.53	186.93	10
2017	August	7.24	32.50	74.18	159.67	283.74	24
2017	September	0.61	8.79	31.48	88.08	156.47	2
2017	October	0.08	0.82	2.20	4.98	11.06	2
2017	November	0.00	0.00	0.00	0.00	0.14	0
2018	April	1.66	5.26	11.54	22.25	34.30	0
2018	May	1.73	3.22	5.73	9.18	13.21	1
2018	June	1.57	5.81	10.52	22.29	32.89	6
2018	July	13.74	29.99	48.04	74.34	98.01	7
2018	August	37.83	71.67	109.27	157.55	201.00	29
2018	September	54.55	82.03	112.57	147.58	179.09	24
2018	October	2.13	2.90	3.77	5.89	7.80	6
2018	November	0.00	0.00	0.00	0.08	0.15	0

Table 7: Model validation for *Aedes koreicus* model in Trento (NE Italy)